Chemical Product and Process Modeling

Volume 6, *Issue* 1 2011 *Article* 11

Structured Model of VERO Cells Metabolism in a Fixed-Bed Bioreactor

Valérie Gelbgras, *Université Libre de Bruxelles*
Christophe E. Wylock, *Université Libre de Bruxelles*
Jean-Christophe Drugmand, *Artelis S.A.*
Benoît Haut, *Université Libre de Bruxelles*

Recommended Citation:
Gelbgras, Valérie; Wylock, Christophe E.; Drugmand, Jean-Christophe; and Haut, Benoît (2011) "Structured Model of VERO Cells Metabolism in a Fixed-Bed Bioreactor," *Chemical Product and Process Modeling*: Vol. 6 : Iss. 1, Article 11.
Available at: http://www.bepress.com/cppm/vol6/iss1/11
DOI: 10.2202/1934-2659.1534

Structured Model of VERO Cells Metabolism in a Fixed-Bed Bioreactor

Valérie Gelbgras, Christophe E. Wylock, Jean-Christophe Drugmand, and Benoît Haut

Abstract

In this work, a structured mathematical model of the VERvet Origin (VERO) cell metabolism in a fixed-bed bioreactor is developed. Mass balance equations for the extra- and intracellular species are written considering the main pathways of the animal cell metabolism. From the model equations, an undetermined set of equations relating the consumption or production velocities of the extracellular species and the velocities of the metabolic reactions can be developed. The monitoring of a reference cell culture enables to transform this undetermined set of equations in a determined one. The resolution of this determined set of equations enables to analyze and characterize the cell metabolism. From the model and the cell metabolism characterization, a monitoring tool is developed to simulate the time evolution of the species concentrations when the time evolution of the cell concentration is known. This simulation tool is used to simulate five experimental cell cultures. The comparison of the experimentally determined and computed time evolutions of the species concentrations enables to validate the developed monitoring tool. The validated monitoring tool can be used to optimize the operating conditions of the culture, as the medium feeding rate, the range of the species concentrations.

KEYWORDS: VERO cells, structured model, monitoring tool

Author Notes: This work was supported by a grant of the FRIA (Fonds pour la formation à la Recherche dans l'Industrie et dans l'Agriculture).

1. Introduction

Animal cell cultures in a bioreactor are particularly relevant to produce monoclonal antibodies, viral particles … (Blüml 2007; Decker et al. 2007). In this work, the VERvet Origin (VERO) cell cultures in serum free medium are cultivated in a fixed-bed bioreactor of the biotechnological company Artelis S.A.. This bioreactor is called iCELLis. In the iCELLis bioreactor (Figure 1), the cells adhere to the fibers of porous carriers placed in a compartment of the bioreactor, called a fixed-bed (FB). A pump delivers the culture medium through the fixed-bed. The medium carries the nutrients to the adhering cells and evacuates the by-products (Meuwly 2006). At the outlet of the fixed-bed, the medium flows through a gas-liquid mass transfer system (a falling liquid film) in order to be oxygenated. A culture medium feeding system can supply the medium with nutrients. Then, the medium flows again through the fixed-bed.

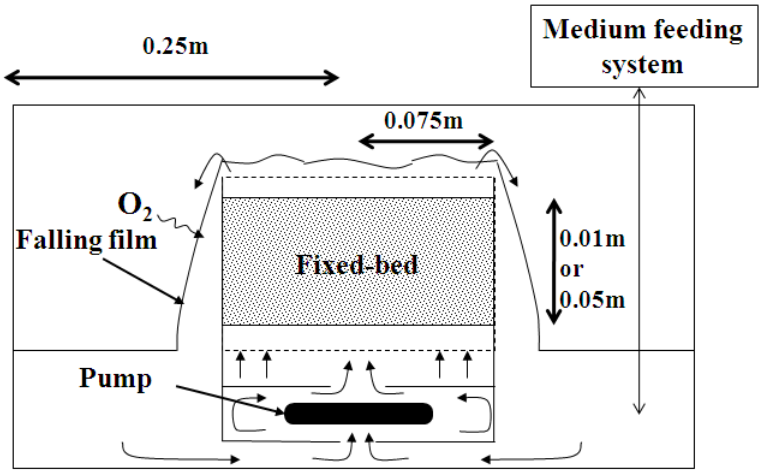

Figure 1 – Block diagram of the iCELLis fixed-bed bioreactor.

The advantages of a fixed-bed bioreactor are the high cell concentration, the cell retention with a weak cell exposition to the shear stresses, the easiness of the medium perfusion ... Nevertheless, a fixed-bed bioreactor presents some drawbacks, for instance, the presence of the cell concentration gradients along the fixed-bed and a difficult monitoring of the extracellular species concentrations in the fixed-bed during the process (Fassnacht et al. 1999; Warnock et al. 2005).

In another work (Gelbgras et al. 2010), a model has been successively developed to evaluate the cell concentration gradients in the fixed-bed and to optimize the fixed-bed bioreactor. To complete this work, the developed model requires a coupling to a model of the cell metabolism. An efficient optimization of the fixed-bed bioreactor can be achieved through an excellent understanding of

the cell metabolism. Indeed, the selection of some operating parameters as the flow rate, the medium composition, the profile of the medium feeding rate … is strongly dependent on the cell metabolism. Furthermore, in order to develop the iCELLis bioreactor for an industrial scale, the development of the monitoring tool of the extracellular species concentrations inside of the fixed-bed is fundamental. This paper presents a method to develop a monitoring tool of the extracellular species concentration for an animal cell culture. Develop this monitoring tool requires a model of the animal cell metabolism.

Cell metabolism models can be either unstructured or structured. An ***unstructured*** model is a macroscopic description of the cell metabolism. Such a model characterizes the conversion from an extracellular species to another extracellular species, for instance glucose into lactate or glutamine into ammonia. This kind of model is generally not computer power consuming contrary to the structured model. However, the use of this model as a simulation tool is limited to the experimental field of the model parameters identification. The extrapolation to another experimental field is often risky (Jang et al. 2000). A ***structured*** model requires more equations and deeper biological knowledge of the cell metabolism than the unstructured model. In this kind of model, the intracellular metabolic reactions are characterized and connected to the time evolution of the nutrient and by-product concentrations (Sanderson et al. 1999). The extrapolation to another experimental field is often more opportune than with the unstructured model. Moreover, an unstructured model can be built by applying systematic procedures for the complexity reduction of a structured model (Haag et al. 2005).

In this work, the following nomenclature is used:

- the nutrients and by-products are called the extracellular species. Their concentrations are written $C_{\mathrm{ext,i}}$ (number of moles per unit of culture medium volume in $\mathrm{mol/m^3_{MED}}$), with i indicating the considered extracellular species;
- the consumption or production of these extracellular species are characterized by a consumption or production velocities written $v_{\mathrm{ext,i}}$ (number of moles consumed/produced per cell and per time unit in $\mathrm{mol/(cell\ s)}$), with i indicating the considered extracellular species;
- the intracellular metabolites are called the intracellular species. Their concentrations are written $C_{\mathrm{int,j}}$ (number of moles per unit of culture medium volume and per cell in $\mathrm{mol/(m^3_{MED}\ cell)}$), with j indicating the considered intracellular species;
- the rates of the metabolic reactions are written v_{n} (in $\mathrm{mol/(cell\ s)}$) with n indicating the considered metabolic reaction.

DOI: 10.2202/1934-2659.1534

The ***first objective*** of this work is to develop a structured mathematical model of the animal cell metabolism in a fixed-bed bioreactor. For this purpose, the balance equations for the extra- and intracellular species are written considering the main pathways of the animal cell metabolism.

The ***second objective*** of this work is to apply this model to the VERO cells and to analyze their metabolism. For this purpose, from the model equations, a set of equations relating $v_{\mathrm{ext,i}}$ and v_{n} is developed. This set of equations is initially undetermined. A reference cell culture is realized in the iCELLis fixed-bed bioreactor. The monitoring of this reference cell culture enables to transform this undetermined set of equations in a determined one. The resolution of the determined set of equations enables to characterize the cell metabolism of the reference culture.

The ***third objective*** of this work is to develop a monitoring tool to simulate the time evolution of the extracellular species concentrations when the time evolution of the VERO cell concentration in the fixed-bed is known. To achieve this third objective, the time evolutions of $C_{\mathrm{ext,i}}$ and $v_{\mathrm{ext,i}}$ during the reference cell culture are computed with the structured model equations and the analysis of the cell metabolism. The relations between $C_{\mathrm{ext,i}}$ and $v_{\mathrm{ext,i}}$ are identified and introduced in the model equations. Therefore, the model can be used as a simulation tool to predict the time evolution of the species concentrations when the cell concentration in the fixed-bed is known. This simulation tool is used to simulate five cell cultures experimentally realized in the iCELLis fixed-bed bioreactor. The experimentally determined and computed time evolutions of the species concentrations are compared to validate the monitoring tool.

This work is organized as follows. The materials and methods used in this work are presented in section 2. The results are discussed in section 3. Finally, section 4 concludes the obtained results.

2. Materials and methods

2.1. Structured model of the animal cell metabolism in the fixed-bed bioreactor

2.1.1. Assumptions and pathways of the cell metabolism

The height of the fixed-bed (H_{FB}) equals 10^{-2} or $5\ 10^{-2}$m. In this range of H_{FB}, the adhering cell concentration can be assumed homogeneous (Gelbgras et al. 2010). The characteristic time of the production or the consumption of the extracellular species is assumed much larger than the residence time of the medium in the fixed-bed. Therefore, the species concentration gradients in the bioreactor are not significant.

The network of the metabolic reactions is reduced to the main metabolic pathways of the animal cells. The modeled network of the metabolic reactions is schematically presented in Figure 2. The main pathways of the animal cell metabolism are the lactate fermentation, the glycolysis, the tricarboxylic acid (TCA) cycle, the pentose phosphate pathway, the aminotransferase pathway and the synthesis of the animal cell (Provost et al. 2004; Drugmand 2007). A reaction rate written v_n (in $\mathrm{mol}/(\mathrm{cell\ s})$, n indicates the reaction) is associated to each considered reaction. If the reaction rate is positive, the reaction direction is indicated by the arrow in Figure 2, otherwise it is in the other direction.

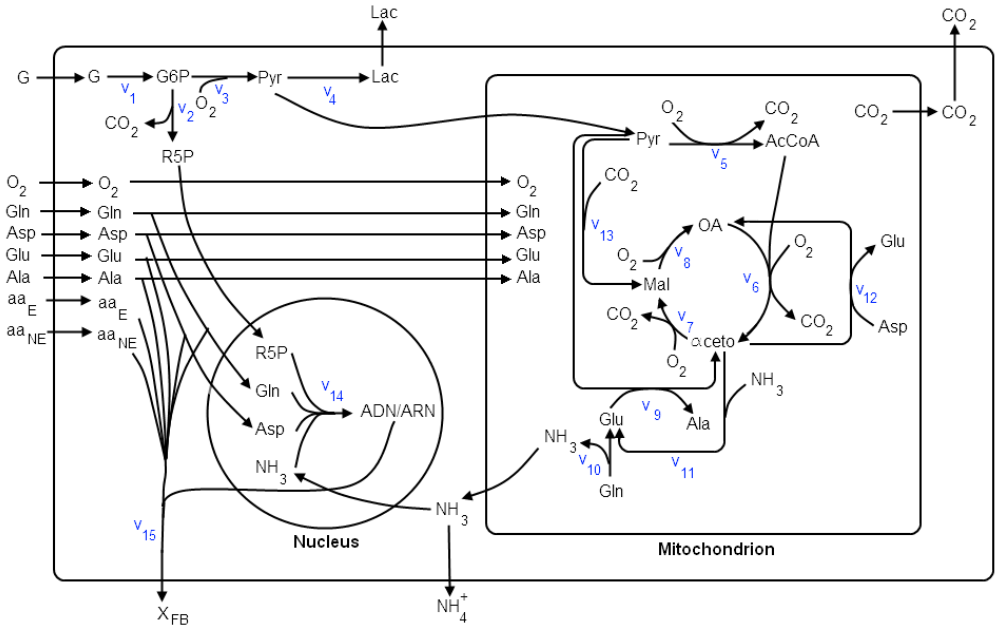

Figure 2 – Modeled network of the metabolic reactions. Glucose (G), glutamine (Gln), glutamate (Glu), aspartate (Asp), alanine (Ala), other non essential amino acid (aa_{NE}), essential amino acid (aa_E), ammonium/ammonia (NH_4^+/NH_3), lactate (Lac), oxygen (O_2), carbon dioxide (CO_2), glucose-6 phosphate (G6P), ribose-5-phosphate (R5P), pyruvate (Pyr), acetyl coenzyme A (AcCoA), oxaloacetate (OA), α-cetoglutarate (αceto), malate (Mal), nucleic acid (ADN/ARN) and the cell (X_{FB}).

Glucose (G), glutamine (Gln), glutamate (Glu), aspartate (Asp), alanine (Ala), other non essential amino acid (aa_{NE}), essential amino acid (aa_E) and oxygen are transported through the plasma membrane into the cell (Kilberg et al. 1992; Gartner et al. 2007).

In the cell, glucose is transformed into glucose-6-phosphate (G6P) by the glycolysis (Eq. (1)). The required energy for this reaction is given by the hydrolysis of adenosine triphosphate (ATP) into adenosine diphosphate (ADP).

DOI: 10.2202/1934-2659.1534

$$\mathrm{G} + \mathrm{ATP} \xrightarrow{v_1} \mathrm{G6P} + \mathrm{ADP} \quad (1)$$

Glucose-6-phosphate is transformed into ribose-5-phosphate (R5P) by the pentose phosphate pathway (Eq. (2)). This reaction is coupled to the reduction of the nicotinamide adenine dinucleotide phosphate ($\mathrm{NADP^+/NADPH}$). Glucose-6-phosphate can also be transformed into pyruvate (Pyr) by the glycolysis (Eq. (3) where P_i is inorganic phosphate) (Lehningher 1977).

$$\mathrm{G6P} + 2\mathrm{NADP^+} + \mathrm{H_2O} \xrightarrow{v_2} \mathrm{R5P} + 2\mathrm{NADPH} + 2\mathrm{H^+} + \mathrm{CO_2} \quad (2)$$

$$\mathrm{G6P} + 7\mathrm{ADP} + 6\mathrm{P_i} + O_2 \xrightarrow{v_3} 2\mathrm{Pyr} + 7\mathrm{ATP} + 2\mathrm{H_2O} \quad (3)$$

Pyruvate is an intermediate species of two pathways (Seth et al. 2006). In the lactic fermentation, pyruvate is transformed in lactate (Lac). This transformation is coupled to the oxidation of nicotinamide adenine dinucleotide ($\mathrm{NADH/NAD^+}$) (Eq. (4)). By the glycolysis, pyruvate, coenzyme A (CoASH) and oxygen react to form acetyl coenzyme A (AcCoA) and carbon dioxide (Eq. (5)). In this reaction, ATP is produced.

$$\mathrm{Pyr} + \mathrm{NADH} + \mathrm{H^+} \xrightarrow{v_4} \mathrm{Lac} + \mathrm{NAD^+} \quad (4)$$

$$\mathrm{Pyr} + \mathrm{CoASH} + 3\mathrm{ADP} + 3\mathrm{P_i} + \frac{1}{2}\mathrm{O_2} \xrightarrow{v_5} \mathrm{AcCoA} + \mathrm{H_2O} + \mathrm{CO_2} + 3\mathrm{ATP} \quad (5)$$

By the TCA cycle, acetyl coenzyme A, oxaloacetate (OA) and oxygen react to form α-cetoglutarate (αceto), carbon dioxide and coenzyme A (Eq. (6)). Then, α-cetoglutarate is oxydated in malate (Mal) (Eq. (7). Malate can be also oxydated to reform oxaloacetate (Eq. (8)). In these three reactions, ATP is produced.

$$\mathrm{AcCoA} + \mathrm{OA} + \frac{1}{2}\mathrm{O_2} + 3\mathrm{ADP} + 3\mathrm{P_i} \xrightarrow{v_6} \alpha\mathrm{ceto} + \mathrm{CO_2} + \mathrm{CoASH} + 3\mathrm{ATP} \quad (6)$$

$$\alpha\mathrm{ceto} + \mathrm{O_2} + 6\mathrm{ADP} + 6\mathrm{P_i} \xrightarrow{v_7} \mathrm{Mal} + \mathrm{H_2O} + \mathrm{CO_2} + 6\mathrm{ATP} \quad (7)$$

$$\mathrm{Mal} + \frac{1}{2}\mathrm{O_2} + 3\mathrm{ADP} + 3\mathrm{P_i} \xrightarrow{v_8} \mathrm{OA} + \mathrm{H_2O} + \mathrm{CO_2} + 3\mathrm{ATP} \quad (8)$$

Some intermediate species of the TCA cycle participate also in the amino-transferase pathway (Lehningher 1977; Voet et al. 2005; Champe et al. 2008). Pyruvate and glutamate react to form α-cetoglutarate and alanine (Eq. (9)).

Glutamine decomposes into glutamate and ammonium (Eq. (10)). α-cetoglutarate and ammonium react to form glutamate (Eq. (11)). Aspartate and α-cetoglutarate react to form oxaloacetate and glutamate (Eq. (12)).

$$\mathrm{Pyr} + \mathrm{Glu} \xrightarrow{v_9} \alpha\mathrm{ceto} + \mathrm{Ala} \tag{9}$$

$$\mathrm{Gln} + \mathrm{H_2O} \xrightarrow{v_{10}} \mathrm{Glu} + \mathrm{NH_3} \tag{10}$$

$$\alpha\mathrm{ceto} + \mathrm{NH_3} + \mathrm{NADPH} + \mathrm{H^+} \xrightarrow{v_{11}} \mathrm{Glu} + \mathrm{NADP^+} + \mathrm{H_2O} \tag{11}$$

$$\mathrm{Asp} + \alpha\mathrm{ceto} \xrightarrow{v_{12}} \mathrm{OA} + \mathrm{Glu} \tag{12}$$

Pyruvate can also be transformed into malate (Eq. (13)).

$$\mathrm{Pyr} + \mathrm{CO_2} + \mathrm{NADPH} + \mathrm{H^+} \xrightarrow{v_{13}} \mathrm{Mal} + \mathrm{NADP^+} \tag{13}$$

To simplify the equation of the synthesis of an animal cell, such a cell is assumed to be only composed of proteins ($117\ 10^{-14}\mathrm{mol_{protein}/cell}$) and of nucleic acids ($13\ 10^{-14}\mathrm{mol_{ADN/ARN}/cell}$), as they represent 76.5% of the dry weight of the cell (Zupke et al. 1995; Martens 2007). Therefore, the cells are composed of $7.04\ 10^{11}\ \mathrm{mol_{protein}/mol_{cell}}$ and of $7.83\ 10^{10}\mathrm{mol_{ADN/ARN}/mol_{cell}}$.

The nucleic acids of the animal cells are composed of 66.9% of ADN and of 33.1% of ARN (Zupke et al. 1995). The ADN and the ARN are composed of purine and pyridine in the following proportions: 50% of purine and 50% of pyridine for ADN, 48.8% of purine and 51.2% of pyridine for the ARN, as presented in Figure 3 (Darnell 1968). The equations of the synthesis of the purine and pyridine, (computed by Drugmand 2007) are given by Eq. (14) and Eq. (15), respectively. Using Eq. (14), Eq. (15) and the proportion indicated in Figure 3, the stoichiometric equation of the nucleic acids synthesis can be determined (Eq. (16)).

$$1.79\mathrm{Gln} + 1.32\mathrm{Asp} + \mathrm{ATP} + \mathrm{R5P} + 0.25\mathrm{NH_3} \rightarrow \mathrm{purine} \tag{14}$$

$$2.11\mathrm{Gln} + 1.32\mathrm{Asp} + \mathrm{ATP} + \mathrm{R5P} + 0.25\mathrm{NH_3} \rightarrow \mathrm{pyridine} \tag{15}$$

$$1.95\mathrm{Gln} + 1.32\mathrm{Asp} + \mathrm{ATP} + \mathrm{R5P} + 0.25\mathrm{NH_3} \xrightarrow{v_{14}} \mathrm{ADN/ARN} \tag{16}$$

DOI: 10.2202/1934-2659.1534

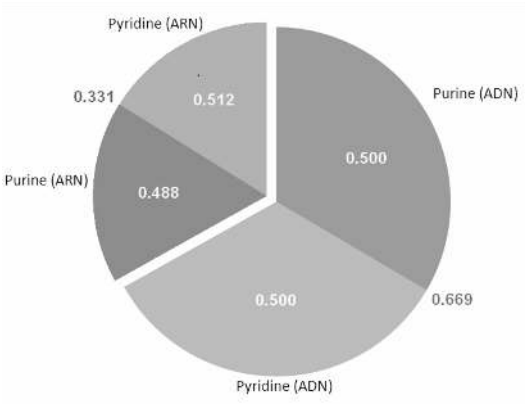

Figure 3 – Composition of the nucleic acids.

The proteins are composed of amino acids. The proportions of amino acids in the animal cell proteins are presented in Table 1 (Okayasu et al. 1997). With these proportions and the proportion of the proteins in the cells, the stoichiometric coefficients of the amino acids in the equation of the cell synthesis can be determined (Eq. (17) where X_{FB} is the adhering cell concentration in the fixed-bed: number of cells by volume unit of the fixed-bed in $\mathrm{cell}/\mathrm{m}^3_{\mathrm{FB}}$, V_{FB} is the fixed-bed volume in $\mathrm{m}^3_{\mathrm{FB}}$, and N_{A} is the Avogadro number). The stoichiometric coefficients of Eq. (17) are expressed for one mole of cells, thus $N_{\mathrm{A}}\mathrm{cells}$. The energy required to synthesize the cell is unknown. Therefore, the stoichiometric coefficient of the ATP in Eq. (17) is undetermined (β). The reaction rate for the cell synthesis (v_{15}) can be expressed by Eq. (18).

$$2.90\ 10^{11}\mathrm{aa_E} + 2.55\ 10^{11}\mathrm{aa_{NE}} + 2.75\ 10^{10}\mathrm{Gln} + 3.80\ 10^{10}\mathrm{Asp} + 5.28\ 10^{10}\mathrm{Ala} + 4.08\ 10^{10}\mathrm{Glu} + 7.83\ 10^{10}\mathrm{ADN/ARN} + \beta\mathrm{ATP} \xrightarrow{v_{15}} X_{\mathrm{FB}}V_{\mathrm{FB}}/N_{\mathrm{A}} \quad (17)$$

$$v_{15}(t) = \frac{1}{N_{\mathrm{A}}X_{\mathrm{FB}}}\frac{dX_{\mathrm{FB}}}{dt} \quad (18)$$

The lactate, the ammonia and the carbon dioxide are transported through the plasma membrane out of the cell.

To summarize, the network of the metabolic reactions modeled in this work contains 15 equations (Eq. (1) to Eq. (13), Eq. (16) and Eq. (17).

Table 1 – Amino acid composition of the proteins of an animal cell (Okayasu et al. 1997).

Alanine	7.5%
Aspartate	5.4%
Glutamine	3.9%
Glutamate	5.8%
aa_{NE}	36.2%
aa_{E}	41.2%

2.1.2. Balance equations of the model

2.1.2.1. Time evolution of the cell concentration and definition of the rate of the cell synthesis

A mass balance for the adhering cell on the bioreactor, using the Verhulst logistic equation, leads to Eq. (19) (Jolivet et al. 1982; Ricklefs et al. 2003). The selection of the Verhulst logistic equation is based on another work (Gelbgras et al. 2010). The cell growth rate is assumed to be first order with respect to X_{FB} and the cell death rate is assumed to be second order with respect to X_{FB}. μ is the specific growth rate of the cells (in s^{-1}). k_D^{eff} is the effective kinetic constant of the cell death rate (in $m_{FB}^3/(\text{cell s})$). If μ and k_D^{eff} are time independent (as for the cell cultures in this work, see sections 3.1.1 and 3.2.2.1), the integration of Eq. (19) from $(t_0, X_{FB,0})$ to (t, X_{FB}) leads to Eq. (20). With this equation, the time evolution of the cell concentration can be modeled during the whole culture without changing the values of μ and k_D^{eff}. The cell concentration increases up to a maximal cell concentration ($X_{FB}^{max,tot}$ in cell/m_{FB}^3) equal to the ratio μ/k_D^{eff}. This maximal cell concentration characterizes the biological limit of the cell to divide and the limit imposed by the specific area of the carriers (Gelbgras et al. 2010).

$$\frac{dX_{FB}}{dt} = \mu X_{FB} - k_D^{eff} X_{FB}^2 \quad \textbf{(19)}$$

$$X_{FB} = \frac{\frac{\mu}{k_D^{eff}}}{1 + \left(\frac{\mu}{k_D^{eff}}\frac{1}{X_{FB,0}} - 1\right) e^{-\mu(t-t_0)}} = \frac{X_{FB}^{max,tot}}{1 + \left(\frac{X_{FB}^{max,tot}}{X_{FB,0}} - 1\right) e^{-\mu(t-t_0)}} \quad \textbf{(20)}$$

2.1.2.2. Time evolution of the extracellular species concentrations

In the model, 11 extracellular species are considered: glucose, glutamine, glutamate, aspartate, alanine, other non essential amino acids, essential amino acids, ammonia, lactate, oxygen and carbon dioxide. The notations for their concentrations are summarized in Table 2.

DOI: 10.2202/1934-2659.1534

Table 2 – Notations for the extracellular species concentrations.

G	→	$C_{\text{ext},1}$	Asp	→	$C_{\text{ext},4}$	aa_E	→	$C_{\text{ext},7}$	O_2	→	$C_{\text{ext},10}$
Gln	→	$C_{\text{ext},2}$	Ala	→	$C_{\text{ext},5}$	Lac	→	$C_{\text{ext},8}$	CO_2	→	$C_{\text{ext},11}$
Glu	→	$C_{\text{ext},3}$	aa_NE	→	$C_{\text{ext},6}$	NH_4^+	→	$C_{\text{ext},9}$			

Mass balances for the extracellular species on the bioreactor lead to Eq. (21) for i = 1 to 9 and to Eq. (22) for i = 10 and 11. The first term of the right-hand side member of these equations characterizes the medium feeding (where $C_{\text{ext,i,feed}}$ is the extracellular species concentration in the medium supplied by the feeding system in $\text{mol}/\text{m}^3_\text{MED}$, Q_feed is the flow rate of the feeding medium in $\text{m}^3_\text{MED}/\text{s}$ and V_MED is the medium volume in the bioreactor in m^3_MED). The second term characterizes the consumption or the production by the cells (where $N_{\text{ext,i-n}}$ is the stoichiometric coefficient of the extracellular species i in the reaction n). In Eq. (22), the third term characterizes the mass transfer in the gas-liquid mass transfer system ($k_\text{L}a$ is the mass transfer coefficient in s^{-1}, a equals the area of gas-liquid interface of the mass transfer system divided the medium volume in the bioreactor, and $C_{\text{ext,i,*}}$ is the saturation concentration of the species i in the medium in $\text{mol}/\text{m}^3_\text{MED}$).

$$\underbrace{\frac{d}{dt}\begin{pmatrix} C_{\text{ext},1} \\ \vdots \\ C_{\text{ext},9} \end{pmatrix}}_{\text{size (9x1)}} = \frac{Q_\text{feed}}{V_\text{MED}}\left(\underbrace{\begin{pmatrix} C_{\text{ext},1,\text{feed}} \\ \vdots \\ C_{\text{ext},9,\text{feed}} \end{pmatrix}}_{\text{size (9x1)}} - \underbrace{\begin{pmatrix} C_{\text{ext},1} \\ \vdots \\ C_{\text{ext},9} \end{pmatrix}}_{\text{size (9x1)}}\right) + \underbrace{\begin{pmatrix} N_{\text{ext},1\text{-}1} & \cdots & N_{\text{ext},1\text{-}15} \\ \vdots & \ddots & \vdots \\ N_{\text{ext},9\text{-}1} & \cdots & N_{\text{ext},9\text{-}15} \end{pmatrix}}_{\text{size (9x15)}} \underbrace{\begin{pmatrix} v_1 \\ \vdots \\ v_{15} \end{pmatrix}}_{\text{size (15x1)}} X_\text{FB}\frac{V_\text{FB}}{V_\text{MED}} \tag{21}$$

$$\underbrace{\frac{d}{dt}\begin{pmatrix} C_{\text{ext},10} \\ C_{\text{ext},11} \end{pmatrix}}_{\text{size (2x1)}} = \frac{Q_\text{feed}}{V_\text{MED}}\left(\underbrace{\begin{pmatrix} C_{\text{ext},10,\text{feed}} \\ C_{\text{ext},11,\text{feed}} \end{pmatrix}}_{\text{size (2x1)}} - \underbrace{\begin{pmatrix} C_{\text{ext},10} \\ C_{\text{ext},11} \end{pmatrix}}_{\text{size (2x1)}}\right) + \underbrace{\begin{pmatrix} N_{\text{ext},10\text{-}1} & \cdots & N_{\text{ext},10\text{-}15} \\ N_{\text{ext},11\text{-}1} & \cdots & N_{\text{ext},11\text{-}15} \end{pmatrix}}_{\text{size (2x15)}} \underbrace{\begin{pmatrix} v_1 \\ \vdots \\ v_{15} \end{pmatrix}}_{\text{size (15x1)}} X_\text{FB}\frac{V_\text{FB}}{V_\text{MED}} + k_\text{L}a\left(\underbrace{\begin{pmatrix} C_{\text{ext},10,*} \\ C_{\text{ext},11,*} \end{pmatrix}}_{\text{size (2x1)}} - \underbrace{\begin{pmatrix} C_{\text{ext},10} \\ C_{\text{ext},11} \end{pmatrix}}_{\textit{size (2x1)}}\right) \tag{22}$$

For the considered metabolic reactions network, the stoichiometric coefficients $N_{\text{ext,i-n}}$ are given in Table 3.

The consumption or production rates of the extracellular species ($v_{\text{ext,i}}$) are given by Eq. (23). The consumption and production rates are negative and positive, respectively.

$$\underbrace{\begin{pmatrix} N_{\text{ext,1-1}} & \cdots & N_{\text{ext,1-15}} \\ \vdots & \ddots & \vdots \\ N_{\text{ext,11-1}} & \cdots & N_{\text{ext,11-15}} \end{pmatrix}}_{\text{size (11x15)}} \underbrace{\begin{pmatrix} v_1 \\ \vdots \\ v_{15} \end{pmatrix}}_{\text{size (15x1)}} = \underbrace{\begin{pmatrix} v_{\text{ext,1}} \\ \vdots \\ v_{\text{ext,11}} \end{pmatrix}}_{\text{size (11x1)}} \quad \textbf{(23)}$$

Table 3 – Stoichiometric coefficients $N_{\text{ext,i-n}}$ for the considered network of the metabolic reactions.

	n														
i	1	2	3	4	5	6	7	8	9	10	11	12	13	14	15
1	-1	0	0	0	0	0	0	0	0	0	0	0	0	0	0
2	0	0	0	0	0	0	0	0	0	-1	0	0	0	-1.95	$-2.75\ 10^{10}$
3	0	0	0	0	0	0	0	0	-1	1	1	1	0	0	$-4.08\ 10^{10}$
4	0	0	0	0	0	0	0	0	0	0	0	-1	0	-1.32	$-3.80\ 10^{10}$
5	0	0	0	0	0	0	0	0	1	0	0	0	0	0	$-5.28\ 10^{10}$
6	0	0	0	0	0	0	0	0	0	0	0	0	0	0	$-2.55\ 10^{10}$
7	0	0	0	0	0	0	0	0	0	0	0	0	0	0	$-2.90\ 10^{10}$
8	0	0	0	1	0	0	0	0	0	0	0	0	0	0	0
9	0	0	0	0	0	0	0	0	0	1	-1	0	0	-0.25	0
10	0	0	-1	0	-0.5	-0.5	-1	-0.5	0	0	0	0	0	0	0
11	0	1	0	0	1	1	1	1	0	0	0	0	-1	0	0

2.1.2.3. Time evolution of the intracellular species concentrations

In the model, 8 intracellular species are considered: glucose-6 phosphate, ribose-5-phosphate, pyruvate, acetyl coenzyme A, oxaloacetate, α-cetoglutarate, malate and ADN/ARN. The notations for their concentrations are summarized in Table 4.

Table 4 – Notations for the intracellular species concentrations.

G6P	→	$C_{\text{int,1}}$	AcCoA	→	$C_{\text{int,4}}$	Mal	→	$C_{\text{int,7}}$
R5P	→	$C_{\text{int,2}}$	OA	→	$C_{\text{int,5}}$	ADN/ARN	→	$C_{\text{int,8}}$
Pyr	→	$C_{\text{int,3}}$	αceto	→	$C_{\text{int,6}}$			

Mass balances for the intracellular species on the bioreactor lead to Eq. (24) (where $N_{\text{int,j-n}}$ is the stoichiometric coefficient of the species j in the reaction n). These balance equations can be transformed into Eq. (25) if Eq. (19) is used. The second term of the right-hand side member of Eq. (25) is assumed negligible compared to the first term. Furthermore, the steady state of $C_{\text{int,j}}$ is assumed. These two assumptions are commonly taken for granted in the literature (Heinrich et al. 1996; Klamt et al. 2003; Rios-Estepa et al. 2007). Therefore, Eq. (25) simplifies in Eq. (26).

DOI: 10.2202/1934-2659.1534

For the considered network of the metabolic reactions, the stoichiometric coefficients $N_{\text{int,j-n}}$ are given in Table 5.

$$\frac{d}{dt}\left(\underbrace{\begin{pmatrix} C_{\text{int},1} \\ \vdots \\ C_{\text{int},8} \end{pmatrix}}_{\text{size (8x1)}} X_{\text{FB}} V_{\text{FB}}\right) = \underbrace{\begin{pmatrix} N_{\text{int},1\text{-}1} & \cdots & N_{\text{int},1\text{-}15} \\ \vdots & \ddots & \vdots \\ N_{\text{int},8\text{-}1} & \cdots & N_{\text{int},8\text{-}15} \end{pmatrix}}_{\text{size (8x15)}} \underbrace{\begin{pmatrix} v_1 \\ \vdots \\ v_{15} \end{pmatrix}}_{\text{size (15x1)}} X_{\text{FB}} \frac{V_{\text{FB}}}{V_{\text{MED}}} \tag{24}$$

$$\begin{aligned} \underbrace{\frac{d}{dt}\begin{pmatrix} C_{\text{int},1} \\ \vdots \\ C_{\text{int},8} \end{pmatrix}}_{\text{size (8x1)}} &= \underbrace{\begin{pmatrix} N_{\text{int},1\text{-}1} & \cdots & N_{\text{int},1\text{-}15} \\ \vdots & \ddots & \vdots \\ N_{\text{int},8\text{-}1} & \cdots & N_{\text{int},8\text{-}15} \end{pmatrix}}_{\text{size (8x15)}} \underbrace{\begin{pmatrix} v_1 \\ \vdots \\ v_{15} \end{pmatrix}}_{\text{size (15x1)}} \frac{1}{V_{\text{MED}}} \\ &\quad - \underbrace{\begin{pmatrix} C_{\text{int},1} \\ \vdots \\ C_{\text{int},8} \end{pmatrix}}_{\text{size (8x1)}} \left(\mu - k_{\text{D}}^{\text{eff}} X_{\text{FB}}\right) \end{aligned} \tag{25}$$

$$\underbrace{\begin{pmatrix} N_{\text{int},1\text{-}1} & \cdots & N_{\text{int},1\text{-}15} \\ \vdots & \ddots & \vdots \\ N_{\text{int},8\text{-}1} & \cdots & N_{\text{int},8\text{-}15} \end{pmatrix}}_{\text{size (8x15)}} \underbrace{\begin{pmatrix} v_1 \\ \vdots \\ v_{15} \end{pmatrix}}_{\text{size (15x1)}} = \underbrace{\begin{pmatrix} 0 \\ \vdots \\ 0 \end{pmatrix}}_{\text{size (8x1)}} \tag{26}$$

Table 5 – Stoichiometric coefficients $N_{\text{int,j-n}}$ for the considered network of the metabolic reactions.

	n														
j	1	2	3	4	5	6	7	8	9	10	11	12	13	14	15
1	1	-1	-1	0	0	0	0	0	0	0	0	0	0	0	0
2	0	1	0	0	0	0	0	0	0	0	0	0	0	-1	0
3	0	0	2	-1	-1	0	0	0	-1	0	0	0	-1	0	0
4	0	0	0	0	1	-1	0	0	0	0	0	0	0	0	0
5	0	0	0	0	0	-1	0	1	0	0	0	1	0	0	0
6	0	0	0	0	0	1	-1	0	1	0	-1	-1	0	0	0
7	0	0	0	0	0	0	1	-1	0	0	0	0	1	0	0
8	0	0	0	0	0	0	0	0	0	0	0	0	0	1	$-7.83\ 10^{10}$

2.2. Analysis of the cell metabolism

2.2.1. Set of equations relating $v_{\text{ext,i}}$ and v_{n}

From the balance equations presented in section 0, a set of equations relating $v_{\text{ext,i}}$ and v_{n} is determined. Eq. (23) and Eq. (26) can be combined, leading to Eq. (27). This set of equations is composed of 19 equations with 26 unknown velocities (15 v_{n} and 11 $v_{\text{ext,i}}$). The following of a reference cell culture enables to determine experimentally six unknown velocities (v_{15} and $v_{\text{ext,i}}$ for i equal to 1, 2, 3, 8 and 9,

see sections 2.2.2 and 2.2.3). The experimental conditions of this reference cell culture are presented in section 2.4. With the knowledge of these velocities, the set of equations is composed of 19 equations with 20 unknown velocities. A supplementary equation has to be considered in order to transform this undetermined set in a determined one.

$$\underbrace{\begin{pmatrix} N_{\text{int,1-1}} & \cdots & N_{\text{int,1-15}} \\ \vdots & \ddots & \vdots \\ N_{\text{int,8-15}} & \cdots & N_{\text{int,8-15}} \\ N_{\text{ext,1-15}} & \cdots & N_{\text{ext,1-15}} \\ \vdots & \ddots & \vdots \\ N_{\text{ext,11-15}} & \cdots & N_{\text{ext,11-15}} \end{pmatrix}}_{\text{size (19x15)}} \underbrace{\begin{pmatrix} v_1 \\ \vdots \\ v_{15} \end{pmatrix}}_{\text{size (15x1)}} = \underbrace{\begin{pmatrix} 0 \\ \vdots \\ 0 \\ v_{\text{ext,1}} \\ \vdots \\ v_{\text{ext,11}} \end{pmatrix}}_{\text{size (19x1)}} \tag{27}$$

To develop this supplementary equation, the global respiration quotient (RQ) is defined as the ratio of the production velocity of CO_2 and the consumption velocity of O_2 (Eq. (28)). The oxidation of glutamine (metabolic reaction 10) and pyruvate implied in the TCA cycle (metabolic reaction 5) are characterized by a RQ equal to $5/6$ and 1, respectively (Bonarius et al. 1996; Xiu et al. 1999). Therefore, if the respiration quotient is considered weighted by consumed glutamine and pyruvate implied in the TCA cycle, a relation between $v_{\text{ext,10}}$, $v_{\text{ext,11}}$, v_{10} and v_5 can be defined (Eq. (28)).

$$\text{RQ} = -\frac{v_{\text{ext,11}}}{v_{\text{ext,10}}} = \frac{v_{10}}{v_5 + v_{10}}\frac{5}{6} + \frac{v_5}{v_5 + v_{10}} \tag{28}$$

If Eq. (28) is joined to the set of equations composed of 19 equations with 20 unknown velocities (Eq. (27)), the resulting set of equations is determined. Therefore, this set of equation can be solved. The solution of this set gives the values of the unknown velocities. These values are specific to the cells of the reference cell culture (VERO cells in this paper). With these values, the cell metabolism can be analyzed and characterized.

2.2.2. Experimental determination of v_{15}

During the reference culture, the time evolution of the adhering cell concentration is followed. For given values of μ and $k_{\text{D}}^{\text{eff}}$, the time evolution of the cell concentration can be computed with Eq. (20). The values of μ and $k_{\text{D}}^{\text{eff}}$ are adjusted to minimize the sum of the quadratic differences between the computed

DOI: 10.2202/1934-2659.1534

and the experimentally determined X_{FB}. Then, the time evolution of v_{15} is determined using Eq. (18).

2.2.3. Experimental determination of the consumption or production rates $\boldsymbol{v}_{\mathrm{ext,1}}$, $\boldsymbol{v}_{\mathrm{ext,2}}$, $\boldsymbol{v}_{\mathrm{ext,3}}$, $\boldsymbol{v}_{\mathrm{ext,8}}$ and $\boldsymbol{v}_{\mathrm{ext,9}}$

The experimental determination of the consumption or production velocities $\boldsymbol{v}_{\mathrm{ext,1}}$, $\boldsymbol{v}_{\mathrm{ext,2}}$, $\boldsymbol{v}_{\mathrm{ext,3}}$, $\boldsymbol{v}_{\mathrm{ext,8}}$ and $\boldsymbol{v}_{\mathrm{ext,9}}$ is realized for the reference cell culture. These velocities are assumed to follow a third order polynomial function with respect to the time (Eq. (29)). $p_{\mathrm{i,3}}$, $p_{\mathrm{i,2}}$, $p_{\mathrm{i,1}}$ and $p_{\mathrm{i,0}}$ are the characteristic parameters of these polynomial functions (in $\mathrm{mol/(cell\,s^4)}$, $\mathrm{mol/(cell\,s^3)}$, $\mathrm{mol/(cell\,s^2)}$ and $\mathrm{mol/(cell\,s)}$, respectively).

The combination of Eq. (21), Eq. (23) and Eq. (29) leads to Eq. (30). Eq. (30) is solved with a program, developed with MatLab 6.5 using a Dormand-Prince algorithm. In this program, the time evolution of X_{FB} is computed with Eq. (20) and the identified values of μ and $k_{\mathrm{D}}^{\mathrm{eff}}$ minimizing the sum of the quadratic differences between the computed and the experimentally determined X_{FB}. The computed time evolutions of the considered $C_{\mathrm{ext,i}}$ are compared to the experimentally determined time evolutions of $C_{\mathrm{ext,i}}$. $p_{\mathrm{i,3}}$, $p_{\mathrm{i,2}}$, $p_{\mathrm{i,1}}$ and $p_{\mathrm{i,0}}$ are adjusted to minimize the sum of the quadratic differences between the computed and the experimentally determined time evolutions of the considered $C_{\mathrm{ext,i}}$. Several polynomial functions for the characterization of the time evolution of $v_{\mathrm{ext,i}}$ have been tested. The third order polynomial function is selected. This order is a good compromise between the number of parameters in the polynomial function and the minimization of the sum of the quadratic differences between the computed and the experimentally determined time evolutions of the $C_{\mathrm{ext,i}}$.

$$\begin{pmatrix} v_{\mathrm{ext,1}}(\mathrm{t}) \\ v_{\mathrm{ext,2}}(\mathrm{t}) \\ v_{\mathrm{ext,3}}(\mathrm{t}) \\ v_{\mathrm{ext,8}}(\mathrm{t}) \\ v_{\mathrm{ext,9}}(\mathrm{t}) \end{pmatrix} = \underbrace{\begin{pmatrix} p_{1,3} \\ p_{2,3} \\ p_{3,3} \\ p_{8,3} \\ p_{9,3} \end{pmatrix}}_{p_{\mathrm{i,3}}} t^3 + \underbrace{\begin{pmatrix} p_{1,2} \\ p_{2,2} \\ p_{3,2} \\ p_{8,2} \\ p_{9,2} \end{pmatrix}}_{p_{\mathrm{i,2}}} t^2 + \underbrace{\begin{pmatrix} p_{1,1} \\ p_{2,1} \\ p_{3,1} \\ p_{8,1} \\ p_{9,1} \end{pmatrix}}_{p_{\mathrm{i,1}}} t + \underbrace{\begin{pmatrix} p_{1,0} \\ p_{2,0} \\ p_{3,0} \\ p_{8,0} \\ p_{9,0} \end{pmatrix}}_{p_{\mathrm{i,0}}} \tag{29}$$

$$\frac{d}{dt}\begin{pmatrix} C_{\mathrm{ext,1}} \\ C_{\mathrm{ext,2}} \\ C_{\mathrm{ext,3}} \\ C_{\mathrm{ext,8}} \\ C_{\mathrm{ext,9}} \end{pmatrix} = \frac{Q_{\mathrm{feed}}}{V_{\mathrm{MED}}}\left(\begin{pmatrix} C_{\mathrm{ext,1,feed}} \\ C_{\mathrm{ext,2,feed}} \\ C_{\mathrm{ext,3,feed}} \\ C_{\mathrm{ext,8,feed}} \\ C_{\mathrm{ext,9,feed}} \end{pmatrix} - \begin{pmatrix} C_{\mathrm{ext,1}} \\ C_{\mathrm{ext,2}} \\ C_{\mathrm{ext,3}} \\ C_{\mathrm{ext,8}} \\ C_{\mathrm{ext,9}} \end{pmatrix}\right) + \begin{pmatrix} v_{\mathrm{ext,1}}(\mathrm{t}) \\ v_{\mathrm{ext,2}}(\mathrm{t}) \\ v_{\mathrm{ext,3}}(\mathrm{t}) \\ v_{\mathrm{ext,8}}(\mathrm{t}) \\ v_{\mathrm{ext,9}}(\mathrm{t}) \end{pmatrix} X_{\mathrm{FB}} \frac{V_{\mathrm{FB}}}{V_{\mathrm{MED}}} \tag{30}$$

During the reference cell culture, the ammonia concentration (i=9) is measured only at $t = 20\text{h}$. Therefore, $p_{9,3}$, $p_{9,2}$, $p_{9,1}$ and $p_{9,0}$ cannot be determined. In the literature, some authors report that if the glutamine consumption rate equals zero, the ammonia production rate equals also zero (Street et al. 1993; Schneider et al. 1996). Therefore, in this work, the ammonia production rate is assumed to be proportional to the glutamine consumption rate (Eq. (31) where γ is a ratio). This ratio is adjusted to minimize the quadratic difference between the computed and the experimentally determined ammonia concentration.

$$v_{\text{ext},9} = \gamma\left(p_{2,3}t^3 + p_{2,2}t^2 + p_{2,1}t + p_{2,0}\right) \tag{31}$$

2.3. Development of a monitoring tool

2.3.1. Relations between $C_{\text{ext,i}}$ and $v_{\text{ext,i}}$

From the time evolutions of $C_{\text{ext,i}}$ and $v_{\text{ext,i}}$ computed in section 2.2.3, the relations $v_{\text{ext,i}}\left(C_{\text{ext,i}}\right)$ are identified. The consumption or production rates of glucose and lactate are related to the glucose concentration. The consumption or production velocities of glutamine, glutamate and ammonia are related to the glutamine concentrations. These selected relations $v_{\text{ext,i}}\left(C_{\text{ext,i}}\right)$ are often mentioned in the literature (Mendonça et al. 1998; Matsuoka et al. 2005; Möhler et al. 2008). These relations are introduced in Eq. (30), leading to Eq. (32). This equation is solved with a program, developed with MatLab 6.5 using a Dormand-Prince algorithm. In this program, the values of μ and $k_{\text{D}}^{\text{eff}}$ are identified with the experimental time evolution of X_{FB}. The identified values of μ and $k_{\text{D}}^{\text{eff}}$ minimize the sum of the quadratic differences between the computed with Eq. (20) and the experimentally determined X_{FB}.

$$\frac{d}{dt}\begin{pmatrix} C_{\text{ext},1} \\ C_{\text{ext},2} \\ C_{\text{ext},3} \\ C_{\text{ext},8} \\ C_{\text{ext},9} \end{pmatrix} = \frac{Q_{\text{feed}}}{V_{\text{MED}}}\left(\begin{pmatrix} C_{\text{ext},1,\text{feed}} \\ C_{\text{ext},2,\text{feed}} \\ C_{\text{ext},3,\text{feed}} \\ C_{\text{ext},8,\text{feed}} \\ C_{\text{ext},9,\text{feed}} \end{pmatrix} - \begin{pmatrix} C_{\text{ext},1} \\ C_{\text{ext},2} \\ C_{\text{ext},3} \\ C_{\text{ext},8} \\ C_{\text{ext},9} \end{pmatrix}\right) + \begin{pmatrix} v_{\text{ext},1}\left(C_{\text{ext},1}\right) \\ v_{\text{ext},2}\left(C_{\text{ext},2}\right) \\ v_{\text{ext},3}\left(C_{\text{ext},2}\right) \\ v_{\text{ext},8}\left(C_{\text{ext},1}\right) \\ v_{\text{ext},9}\left(C_{\text{ext},2}\right) \end{pmatrix} X_{\text{FB}}\frac{V_{\text{FB}}}{V_{\text{MED}}} \tag{32}$$

2.3.2. Monitoring tool validation

During four cell cultures, the time evolutions of the glucose and the lactate concentrations are experimentally followed. During a fifth cell culture, the time evolutions of the glutamate and the ammonia concentrations are experimentally

DOI: 10.2202/1934-2659.1534

determined. During these five cultures for the validation, the time evolutions of the cell concentration are experimentally followed in order to identify the values of μ and $k_{\mathrm{D}}^{\mathrm{eff}}$. The experimental conditions of these cell cultures realized for the model validation are presented in section 2.4.

Considering the operating conditions of these five cell cultures, the time evolutions of $C_{\mathrm{ext,i}}$ are computed with the monitoring tool based on the knowledge of the experimentally determined time evolutions of X_{FB}. The computed time evolutions of $C_{\mathrm{ext,i}}$ are compared to the experimentally determined time evolutions of $C_{\mathrm{ext,i}}$. These comparisons enable to validate the model.

2.4. Animal cell culture in fixed-bed bioreactor

Six cell cultures are realized in the iCELLis fixed-bed bioreactor (Figure 4). The reference cell culture, written R1, is realized to characterize the cell metabolism and develop the monitoring tool. The other cultures, written V1 to V5, are used to validate the monitoring tool.

The radius of the fixed-bed equals $7.5\ 10^{-2}$m. Its height equals 10^{-2} or $5\ 10^{-2}$m. Such heights enable to assume a homogeneous cell concentration in the fixed-bed. The fixed-bed is composed of porous BioNOCII$^{\mathrm{TM}}$ carriers with a pore size between 50 and 200 10^{-6}m. These carriers are placed between two perforated grids (Figure 5). The BioNOCII$^{\mathrm{TM}}$ concentration in the fixed-bed is $132\mathrm{kg/m}_{\mathrm{FB}}^{3}$ (mass of carriers per unit of apparent fixed-bed volume). The volume averaged axial velocity of the medium in the fixed-bed equals $10^{-2}\ \mathrm{m/s}$. In spite of the accumulation of the cell on the carrier, no decreasing of this average velocity is experimentally observed during the cell culture. The temperature is regulated to 36.8°C. The pH is regulated between 7.18 and 7.22. The dissolved oxygen concentration in the medium is regulated around 50% of the saturation concentration (in equilibrium with air).

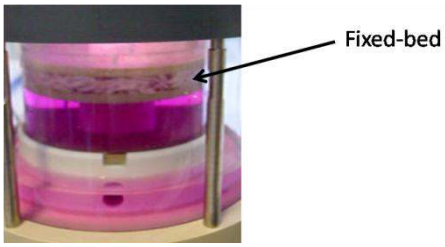

Figure 4 – iCELLis fixed-bed bioreactor.

Figure 5 – BioNOCII$^{\mathrm{TM}}$ carriers (Cesco Bioengineering 2010).

VERO cells are cultivated with OptiPRO$^{\mathrm{TM}}$ Serum Free Medium (Invitrogen 2010) saturated in oxygen and with the addition of glucose and

glutamine. The initial concentrations of glucose ($C_{\text{ext},1,0}$) are given in Table 6. The initial concentration of glutamine ($C_{\text{ext},2,0}$) equals $4\text{mol}/\text{m}^3_{\text{MED}}$. The same concentrations are used in the medium supplied by the feeding system.

The operating conditions of the cell cultures are summarized in Table 7. The time evolutions of the flow rate of the feeding medium for the different cultures are presented in Figure 6.

Table 6 – Concentration of glucose in the initial culture medium and in the culture medium provided by the feeding system.

Culture	$C_{\text{ext},1,0}$ $(\text{mol}/\text{m}^3_{\text{MED}})$	$C_{\text{ext},1,\text{feed}}$ $(\text{mol}/\text{m}^3_{\text{MED}})$
R1	22.5	22.5
V1	21.6	21.6
V2	22.5	22.5
V3	16.5	16.5
V4	16.5	16.5
V5	22.5	22.5

Table 7 – Operating conditions of the cell cultures.

Culture	H_{FB} (10^{-2}m)	V_{MED} $(10^{-3}\text{m}_{\text{MED}})$	$X_{\text{FB},0}$ $(10^{12}\text{cell}/\text{m}^3_{\text{FB}})$
R1	1	1.8	2.24
V1	1	1.8	1.91
V2	1	3.0	3.57
V3	1	1.9	5.50
V4	5	1.9	4.00
V5	5	2.0	10.30

The cell concentration is measured with a biomass sensor placed at the top of the fixed-bed (Cerckel et al. 1993) or on a sample of BioNOCII™ by the crystal violet method (Table 8) (Freshney 2005). The concentrations of glucose, glutamine, glutamate, lactate and ammonia in the medium can be measured in the pump by a BioProfile analyser (Nova Biomedical 2010).

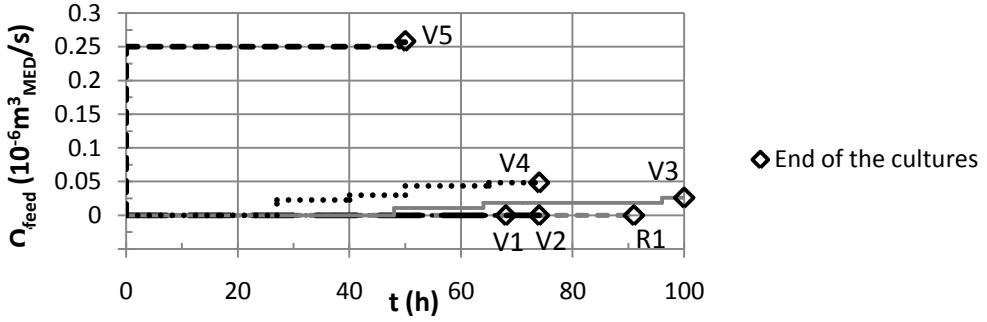

Figure 6 – Time evolutions of the flow rate of the feeding medium.

DOI: 10.2202/1934-2659.1534

Table 8 – Method for the cell concentration measurement.

Culture	Method for the X_{FB} measurement
R1	Crystal violet
V1	Biomass sensor
V2	Crystal violet
V3	Biomass sensor
V4	Biomass sensor
V5	Biomass sensor

3. Results and discussion

3.1. Analysis of the cell metabolism

In order to transform the initial undetermined set of equations in a determined one (see section 2.2.1), the rates v_{15}, $v_{ext,1}$, $v_{ext,2}$, $v_{ext,3}$, $v_{ext,8}$ and $v_{ext,9}$ for the reference cell culture have to be identified.

3.1.1. Experimental determination of v_{15} for the reference cell culture

The experimental time evolution of the cell concentration during the reference cell culture is presented in Figure 7. This figure presents also the computed cell concentration with Eq. (20) using the identified values of μ and k_D^{eff}, by the method described in section 2.2.2. The identified values of μ and k_D^{eff} equal $2.16\ 10^{-2}\mathrm{h}^{-1}$ and $2.10\ 10^{-16}\mathrm{m}_{FB}^3/(\mathrm{cell\ h})$, respectively.

From the identified values of μ and k_D^{eff}, the time evolution of v_{15} can be calculated (Figure 8).

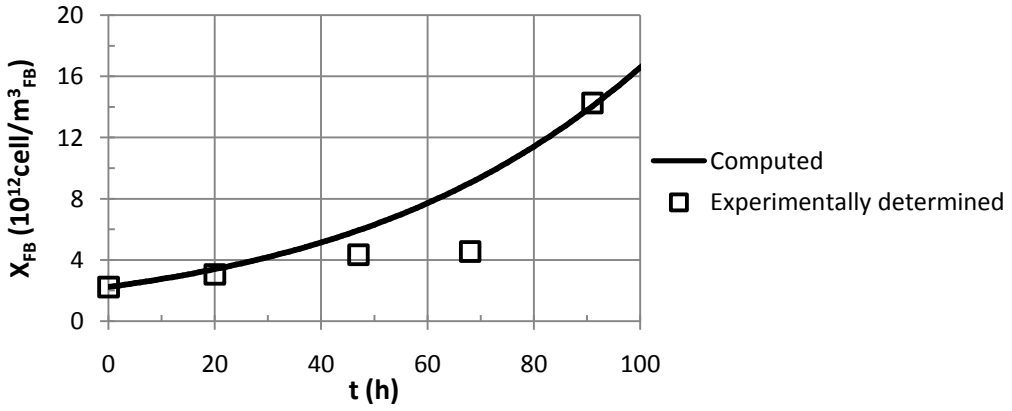

Figure 7 – Computed and experimentally determined time evolutions of the cell concentration. The computed time evolution of X_{FB} is calculated with Eq. (20), using the identified values of μ and k_D^{eff} that minimize the difference between the computed and the experimental X_{FB}.

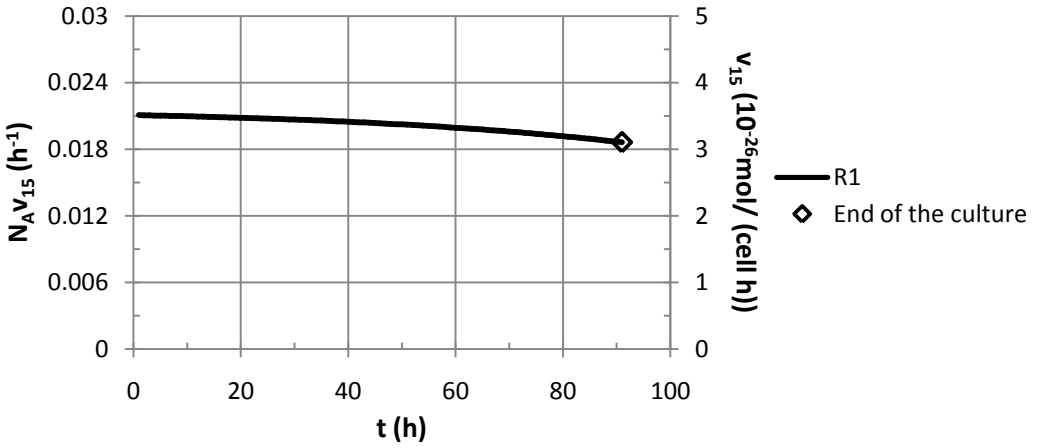

Figure 8 – Time evolution of v_{15} during the reference cell culture.

3.1.2. Experimental determination of the consumption or production rates $v_{ext,1}$, $v_{ext,2}$, $v_{ext,3}$, $v_{ext,8}$ and $v_{ext,9}$ for the reference cell culture

The parameters of the polynomial functions (Eq. (29)) minimizing the sum of the quadratic differences between the computed and the experimentally determined species concentrations for the reference cell culture are presented in Table 9. The identified value of the ratio γ equals -2.2.

Table 9 – Characteristic parameters of the polynomial function modeling the time evolution of the extracellular rates (Eq. (29)). These values minimize the quadratic difference between the computed with Eq. (30) and the experimentally determined time evolutions of the extracellular species concentrations.

i	$p_{i,3}$ (10^{-13}mol/(cell h^4))	$p_{i,2}$ (10^{-13}mol/(cell h^3))	$p_{i,1}$ (10^{-13}mol/(cell h^2))	$p_{i,0}$ (10^{-13}mol/(cell h))
1	$-1.4\ 10^{-6}$	$-5.3\ 10^{-4}$	$1.4\ 10^{-1}$	10
2	$5.7\ 10^{-7}$	$-1.9\ 10^{-4}$	$2.0\ 10^{-2}$	-1.0
3	$-3.1\ 10^{-6}$	$5.9\ 10^{-4}$	$-3.3\ 10^{-2}$	$9.9\ 10^{-1}$
8	$-6.2\ 10^{-6}$	$2.6\ 10^{-3}$	$-3.3\ 10^{-1}$	16
9	$-1.2\ 10^{-6}$	$4.2\ 10^{-4}$	$-4.4\ 10^{-2}$	2.2

DOI: 10.2202/1934-2659.1534

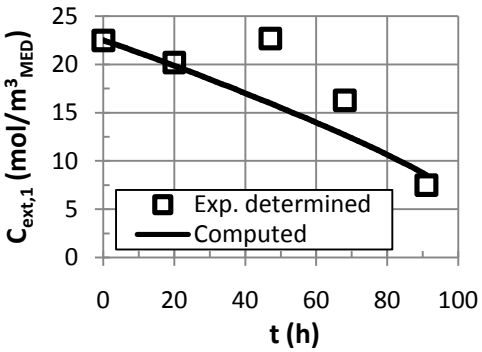

Figure 9 – Computed and experimentally determined time evolutions of the glucose concentration during the reference cell culture. The time evolution of $C_{ext,1}$ is computed with Eq. (29), Eq. (30) and the parameters given in Table 9.

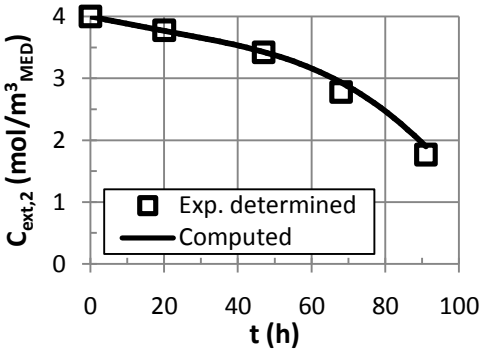

Figure 10 – Computed and experimentally determined time evolutions of the glutamine concentration during the reference cell culture. The time evolution of $C_{ext,2}$ is computed with Eq. (29), Eq. (30) and the parameters given in Table 9.

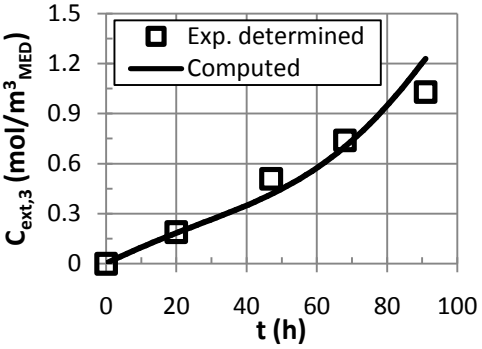

Figure 11 – Computed and experimentally determined time evolutions of the glutamate concentration during the reference cell culture. The time evolution of $C_{ext,3}$ is computed with Eq. (29), Eq. (30) and the parameters given in Table 9.

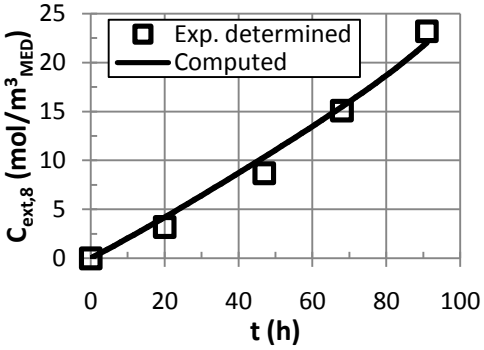

Figure 12 – Computed and experimentally determined time evolutions of the lactate concentration during the reference cell culture. The time evolution of $C_{ext,8}$ is computed with Eq. (29), Eq. (30) and the parameters given in Table 9.

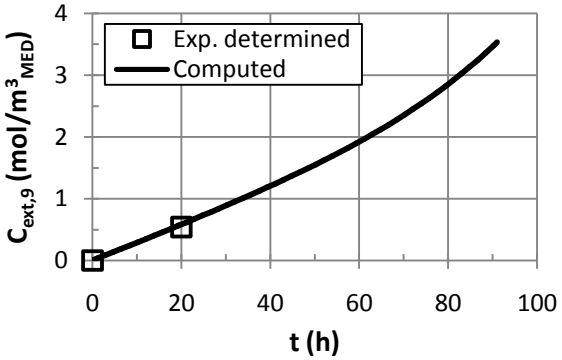

Figure 13 – Computed and experimentally determined time evolutions of the ammonia concentration during the reference cell culture. The time evolution of $C_{ext,9}$ is computed with Eq. (29), Eq. (30) and the parameters given in Table 9.

3.1.3. Resolution of the set of equations relating $v_{\text{ext,i}}$ and v_{n}

As $v_{\text{ext,1}}, v_{\text{ext,2}}, v_{\text{ext,3}}, v_{\text{ext,8}}, v_{\text{ext,9}}$ and v_{15} are known for the reference cell culture (with Eq. (29) and using the parameters given in Table 9), these rates are introduced in the set of equations relating $v_{\text{ext,i}}$ and v_{n} (Eq. (27) and Eq. (28)) to compute the unknown velocities. For instance, the rates at $t = 20,\ 47,\ 68$ and 91h are presented in Table 10.

Table 10 – Computed reaction rates and computed consumption or production rates of the extracellular species for the reference cell culture. The rates are given in 10^{-13}mol/(cell h).

t (h)	20	47	68	91	t (h)	20	47	68	91
v_1	7.500	4.900	3.600	3.000	v_{11}	-0.995	-0.595	-0.480	-0.485
v_2	0.027	0.026	0.026	0.024	v_{12}	2.955	1.510	0.818	0.509
v_3	7.473	4.874	3.574	2.976	v_{13}	-2.881	-1.538	-0.979	-0.684
v_4	10.400	5.600	3.600	2.700	v_{14}	0.027	0.026	0.026	0.024
v_5	5.541	4.742	4.029	3.737	$v_{\text{ext,4}}$	-3.003	-1.557	-0.864	-0.553
v_6	5.541	4.742	4.029	3.737	$v_{\text{ext,5}}$	1.860	0.918	0.474	0.175
v_7	5.467	4.770	4.189	3.911	$v_{\text{ext,6}}$	-0.094	-0.092	-0.089	-0.084
v_8	2.586	3.233	3.210	3.227	$v_{\text{ext,7}}$	-0.091	-0.088	-0.086	-0.081
v_9	1.886	0.943	0.499	0.199	$v_{\text{ext,10}}$	-19.774	-16.002	-13.398	-12.237
v_{10}	0.589	0.350	0.282	0.285	$v_{\text{ext,11}}$	19.458	15.819	13.252	12.092

3.1.4. Analysis of the glucose metabolism

To analyze the glucose metabolism, three ratios are defined to characterize the fraction of the glucose implied in the pentose phosphate pathway ($R_{\text{i=1,n=2}}$, Eq. (33)), in the lactic fermentation ($R_{\text{i=1,n=4}}$, Eq. (34)) and in the TCA cycle ($R_{\text{i=1,n=5}}$, Eq. (35)). These three ratios are calculated for the reference cell culture from the data given in Table 10. The time evolutions of these ratios are presented in Figure 14. As it can be observed, the fraction of the glucose implied in the pentose pathway is negligible compared to the two other fractions (lower than 1%). The glucose is mainly transformed into lactate at the beginning of the culture when the glucose concentration is large. Later during the culture, when the glucose concentration decreases, the fraction of the glucose implied in the TCA cycle increases. This result has been already observed by several authors (Altamirano et al. 2006; Meuwly 2006).

DOI: 10.2202/1934-2659.1534

$$R_{\mathrm{i=1,n=2}} = \frac{v_2}{v_1} \tag{33}$$

$$R_{\mathrm{i=1,n=4}} = \frac{0.5v_4}{v_1} \tag{34}$$

$$R_{\mathrm{i=1,n=5}} = \frac{v_3 - 0.5v_4}{v_1} \tag{35}$$

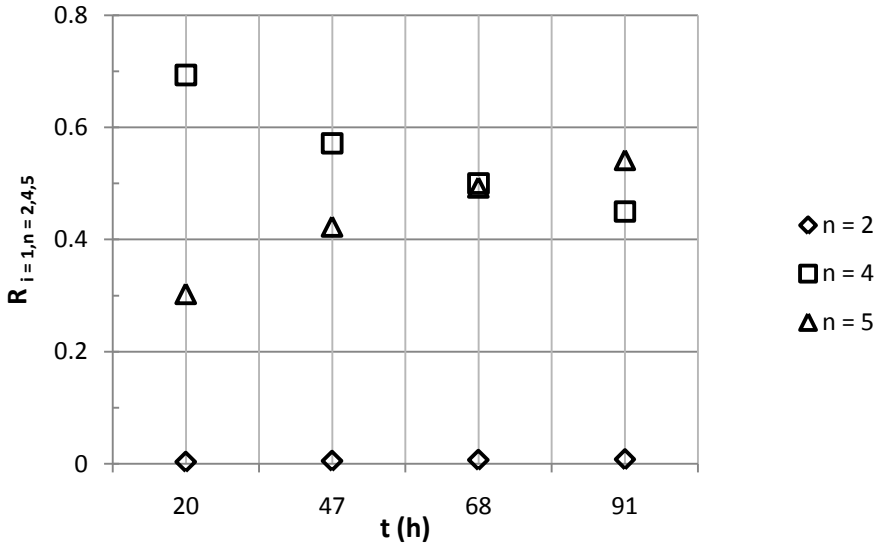

Figure 14 – Fraction of the glucose implied in the pentose phosphate pathway (n = 2), in the lactic fermentation (n = 4) and in TCA cycle (n = 5) for the reference cell culture.

3.1.5. Analysis of the ammonia and glutamate metabolism

The ammonia metabolism is schematically presented in Figure 15. The values of the reaction rate v_{11} identified in Table 10 are negative. Therefore, the reaction is realized in the direction of the transformation of the glutamate in α–cetoglutarate. Indeed, in the literature, it is reported that this transformation is catalyzed by the glutamate deshydrogenase (Huang et al. 2006).

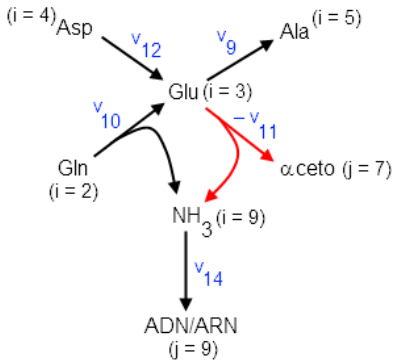

Figure 15 – Metabolism of ammonia from network of the metabolic reactions (presented in Figure 2).

To analyze the ammonia metabolism, a first ratio is defined and written $R_{\mathrm{i=9,n=14}}$ (Eq. (36)). This ratio is the fraction of the intracellular produced ammonia implied in the ADN/ARN synthesis. In Eq. (36), 0.25 is the value of $N_{\mathrm{ext,9\text{-}14}}$. A second ratio is defined and written $R_{\mathrm{i=9,n=12\text{-}11\text{-}ext}}$ (Eq. (37)). This ratio is the fraction of ammonia leaving the cell and produced from aspartate. In Eq. (37), the first term of the right-hand side member is the fraction of intracellular produced ammonia that leaves the cell. The second term is the fraction of intracellular ammonia produced from intracellular glutamate. The last term is the fraction of intracellular glutamate produced from intracellular aspartate. A third ratio is defined and written $R_{\mathrm{i=9,n=10\text{-}ext\,+\,10\text{-}11\text{-}ext}}$ (Eq. (38)). This ratio is the fraction of extracellular ammonia produced from the intracellular glutamine. In Eq. (38), the second term of the right-hand side member is composed of two parts. The first part of this term is the fraction of intracellular ammonia produced from the first decomposition of glutamine. The second part of this term is the fraction of intracellular ammonia produced from intracellular glutamate itself produced from intracellular glutamine. These three ratios are calculated for the reference cell culture from the data given in Table 10 and are presented as a function of the time in Figure 16. The fraction of ammonia implied in the ADN/ARN synthesis is negligible compared to the two other fractions (lower than 1%). A large part of ammonia is produced from the glutamine decomposition. Therefore, the reduction of the ammonia accumulation in the medium should be realized by the diminution of the initial glutamine concentration. Furthermore, the enzymatic activity of the glutamate deshydrogenase, which catalyzes the transformation of the glutamate in α-cetoglutarate, decreases strongly when the glutamine concentration in the medium decreases (Huang et al. 2007). Therefore, a decreasing glutamine concentration enables also to reduce the ammonia produced from the aspartate.

DOI: 10.2202/1934-2659.1534

$$R_{\text{i=9,n=14}} = \frac{0.25v_{14}}{v_{10} - v_{11}} \quad \textbf{(36)}$$

$$R_{\text{i=9,n=12-11-ext}} = \left(1 - \frac{0.25v_{14}}{v_{10} - v_{11}}\right)\frac{-v_{11}}{v_{10} - v_{11}}\frac{v_{12}}{v_{10} + v_{12}} \quad \textbf{(37)}$$

$$R_{\text{i=9,n=10-ext + 10-11-ext}} = \left(1 - \frac{0.25v_{14}}{v_{10} - v_{11}}\right)\left(\frac{v_{10}}{v_{10} - v_{11}} + \frac{v_{10}}{v_{12} + v_{10}}\frac{-v_{11}}{v_{10} - v_{11}}\right) \quad \textbf{(38)}$$

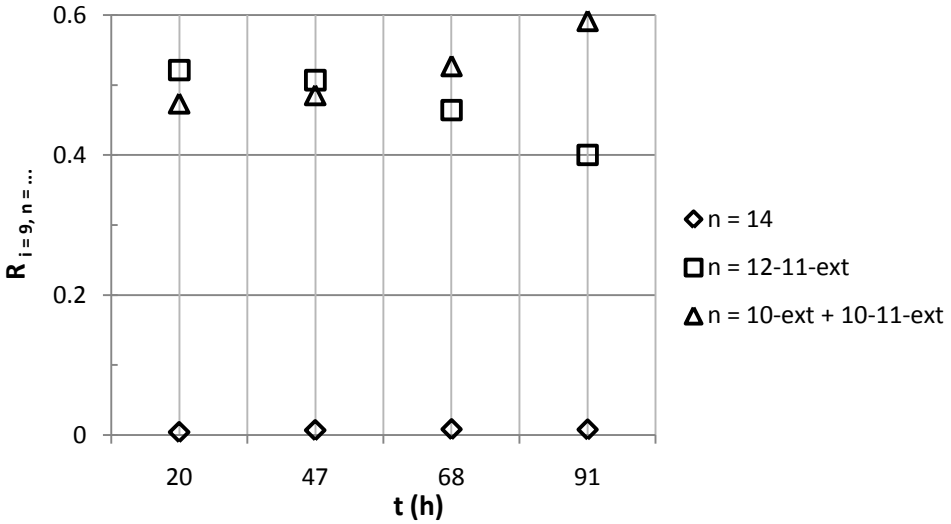

Figure 16 – Time evolution of the fraction of the intracellular produced ammonia implied in the ADN/ARN synthesis (n=14), extracellular ammonia produced from aspartate (n=12-11-ext) and extracellular ammonia produced from glutamine (n=10-ext + 10-11-ext) for the reference cell culture.

3.2. Monitoring tool

3.2.1. Determination of relations between $C_{\text{ext,i}}$ and $v_{\text{ext,i}}$ from the reference cell culture

To develop the monitoring tool, the relations between $C_{\text{ext,i}}$ and $v_{\text{ext,i}}$ are determined from the analysis of the cell metabolism during the reference cell culture. The time evolutions of $C_{\text{ext,i}}$ given in Figure 9 to Figure 13 are related to the time evolutions of $v_{\text{ext,i}}$ computed with Eq. (29) using the parameters values given in Table 9.

$v_{\text{ext,1}}$ and $v_{\text{ext,8}}$ as a function of $C_{\text{ext,1}}$ are presented in Figure 17 for the reference cell culture. The glucose and the lactate concentration ranges equal

$5\text{mol/m}^3_{\text{MED}} < C_{\text{ext,1}} < 22.5\text{mol/m}^3_{\text{MED}}$ and $0\text{mol/m}^3_{\text{MED}} < C_{\text{ext,8}} < 25\text{mol/m}^3_{\text{MED}}$, respectively.

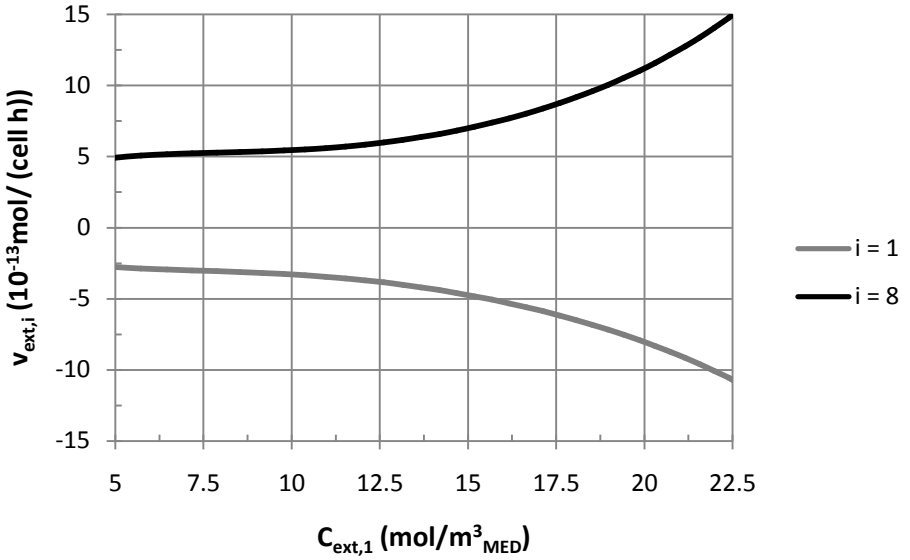

Figure 17 – Glucose consumption rate (i=1) and lactate production rate (i=8) as a function of the glucose concentration. Determination of the relations $v_{\text{ext,1}}(\text{C}_{\text{ext,1}})$ and $v_{\text{ext,8}}(\text{C}_{\text{ext,1}})$ from the reference cell culture.

$v_{\text{ext,2}}$ and $v_{\text{ext,3}}$ as a function of $C_{\text{ext,2}}$ are presented in Figure 18 and Figure 19 for the reference cell culture. During this cell culture, the glutamine and the glutamate concentration ranges equal $1.75\text{mol/m}^3_{\text{MED}} < C_{\text{ext,2}} < 4\text{mol/m}^3_{\text{MED}}$ and $0\text{mol/m}^3_{\text{MED}} < C_{\text{ext,3}} < 1.2\text{mol/m}^3_{\text{MED}}$, respectively. The relation $v_{\text{ext,9}}(\text{C}_{\text{ext,2}})$ is determined from the relation $v_{\text{ext,2}}(\text{C}_{\text{ext,2}})$ and the ratio γ identified in section 2.2.3.

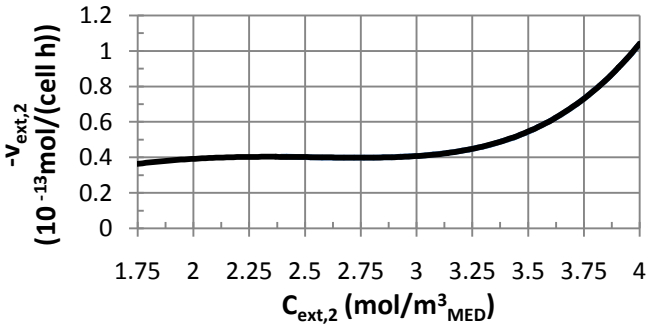

Figure 18 – Consumption velocity of the glutamine (i=2) as a function of the glutamine concentration. Determination of the relation $v_{\text{ext,2}}(\text{C}_{\text{ext,2}})$ from the reference cell culture.

DOI: 10.2202/1934-2659.1534

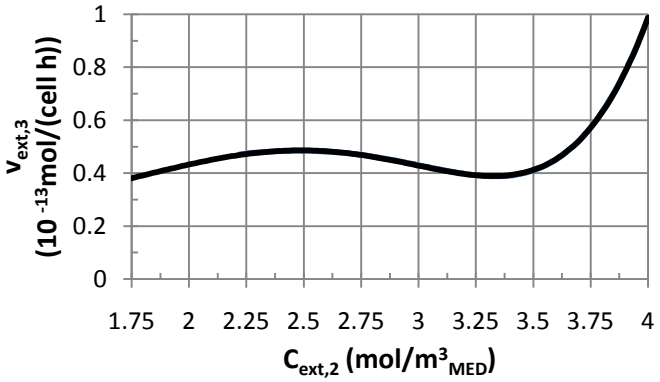

Figure 19 – Production velocity of the glutamate (i=3) as a function of the glutamine concentration. Reference cell culture. Determination of the relation $v_{\text{ext},3}(\mathbf{C}_{\text{ext},2})$ from the reference cell culture.

3.2.2. Monitoring tool validation

3.2.2.1. Experimental determination of v_{15} for the cell culture V1 to V5

The experimental time evolutions of the cell concentration during the five cell cultures V1 to V5 are presented in Figure 20. This figure presents also the computed cell concentration with Eq. (20) using the identified values of μ and $k_{\text{D}}^{\text{eff}}$ that minimize the sum of the quadratic differences between the experimental and the computed cell concentrations (as presented in section 2.2.2). From the identified values of μ and $k_{\text{D}}^{\text{eff}}$ given in Table 11, the time evolution of v_{15} can be calculated (Figure 21).

Table 11 – Identified values of the specific growth rate of the cells and the effective kinetic constant of the cell death rate.

Culture	μ (10^{-2}h^{-1})	$k_{\text{D}}^{\text{eff}}$ $(10^{-16}\text{m}_{\text{FB}}^3/(\text{cell h}))$
V1	2.61	2.10
V2	2.61	2.10
V3	2.58	2.10
V4	1.42	2.10
V5	2.08	2.10

3.2.2.2. Comparison of the computed and experimentally determined time evolution of the $\mathbf{C}_{ext,i}$

The time evolutions of the glucose and lactate concentrations during the cell cultures V1 to V4 are computed with the monitoring tool, based on the knowledge of the experimentally determined time evolution of X_{FB}. These computed time evolutions are compared to the experimentally determined time evolutions (Figure

22). Their good agreement enables to validate the relations $(v_{\text{ext},1}, C_{\text{ext},1})$ and $(v_{\text{ext},8}, C_{\text{ext},1})$ for the studied experimental field.

The time evolutions of the glutamate and the ammonia concentrations during the culture V5 are computed with the monitoring tool, based on the knowledge of the experimentally determined time evolution of X_{FB}. These computed time evolutions are compared to the experimentally determined time evolutions (Figure 23). Their good accordance enables to validate the assumption made in the section 2.2.3 $(v_{\text{ext},9}/v_{\text{ext},2} = \gamma)$. The relations $(v_{\text{ext},3}, C_{\text{ext},2})$ and $v_{\text{ext},9}, C_{\text{ext},2}$ are also validated in for the experimental studied field. The relation $(v_{\text{ext},2}, C_{\text{ext},2})$ is also indirectly validated.

3.2.3. Use the monitoring tool to select the operating conditions of the cell culture

The six cultures present different specific growth rates of the cells (summarized in Table 12). The cultures V1, V2 and V3 present the largest specific growth rates. The reference culture and the culture V5 present similar values of the specific growth rates. The culture V4 presents the smallest specific growth rate.

With the monitoring tool, the time averaged concentrations of glucose, lactate and ammonia are computed for the six cultures (Table 12).
The time averaged concentration of ammonia for the reference culture and the cultures V1 to V3 and V5 are close. During these cultures, the time averaged concentrations of glucose are in a large range. The glucose concentration does not seem directly in relation to the decreasing specific growth rate. The reference

culture and the culture V5 present a larger time averaged concentration of lactate than the culture V1, V2 and V3. Therefore, lactate seems to have an inhibitor effect on the cell growth. For instance, between the culture V3 and V5, an increasing lactate concentration of 26% corresponds to a decreasing specific growth rate of 19% (computed with data given in Table 12). Therefore, a lactate concentration smaller than $12\text{mol}/\text{m}^3_{\text{MED}}$ is more suitable for the cell culture.

The culture V4, with the smallest specific growth rate of the cells, presents the smallest glucose concentration and the largest lactate and ammonia concentration. Ammonia has also an inhibitor effect on the cell growth. The reference culture and the culture V4 present similar ranges of the time averaged concentrations of glucose and lactate. For both of these cultures, an increasing ammonia concentration of 21% corresponds to a decreasing specific growth rate of 34% (computed with data given in Table 12). Therefore, the inhibitor effect of ammonia seems more important than the lactate inhibitor effect. An ammonia concentration smaller than $1.4\text{mol}/\text{m}^3_{\text{MED}}$ is more suitable for the cell culture.

DOI: 10.2202/1934-2659.1534

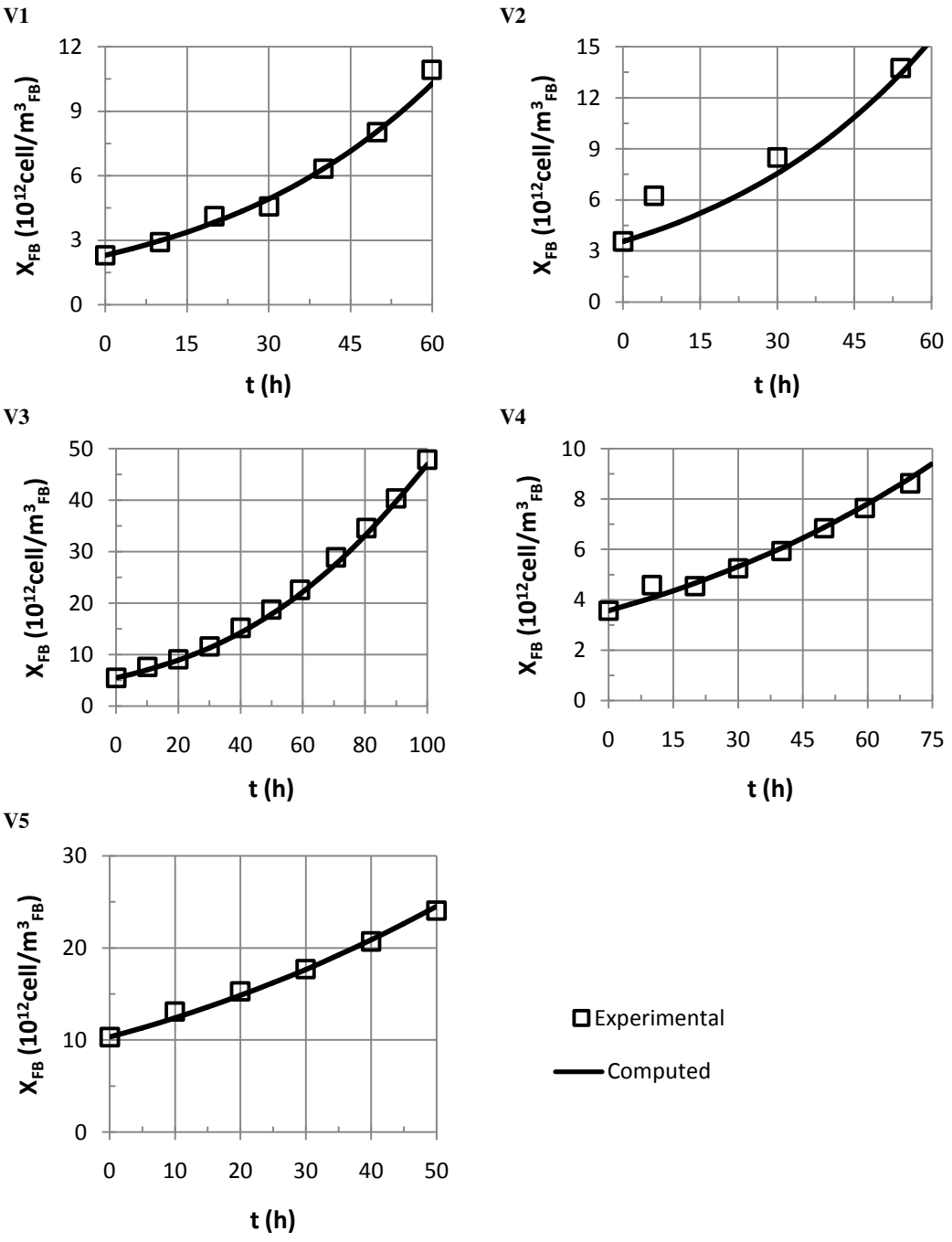

Figure 20 – Experimental and computed time evolutions of the cell concentration. The computed time evolution of X_{FB} is calculated with Eq. (20), using the identified values of μ and k_D^{eff}, minimizing the difference between the computed and the experimental X_{FB}.

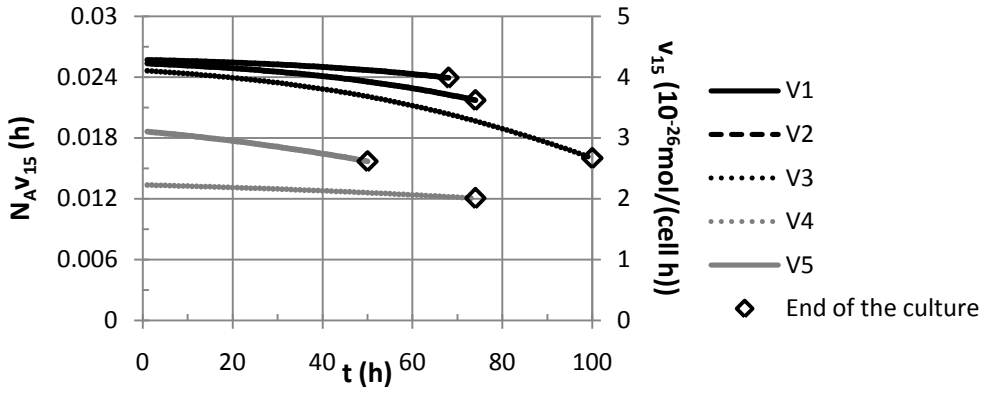

Figure 21 – Time evolution of v_{15} during the cell culture V1 to V5.

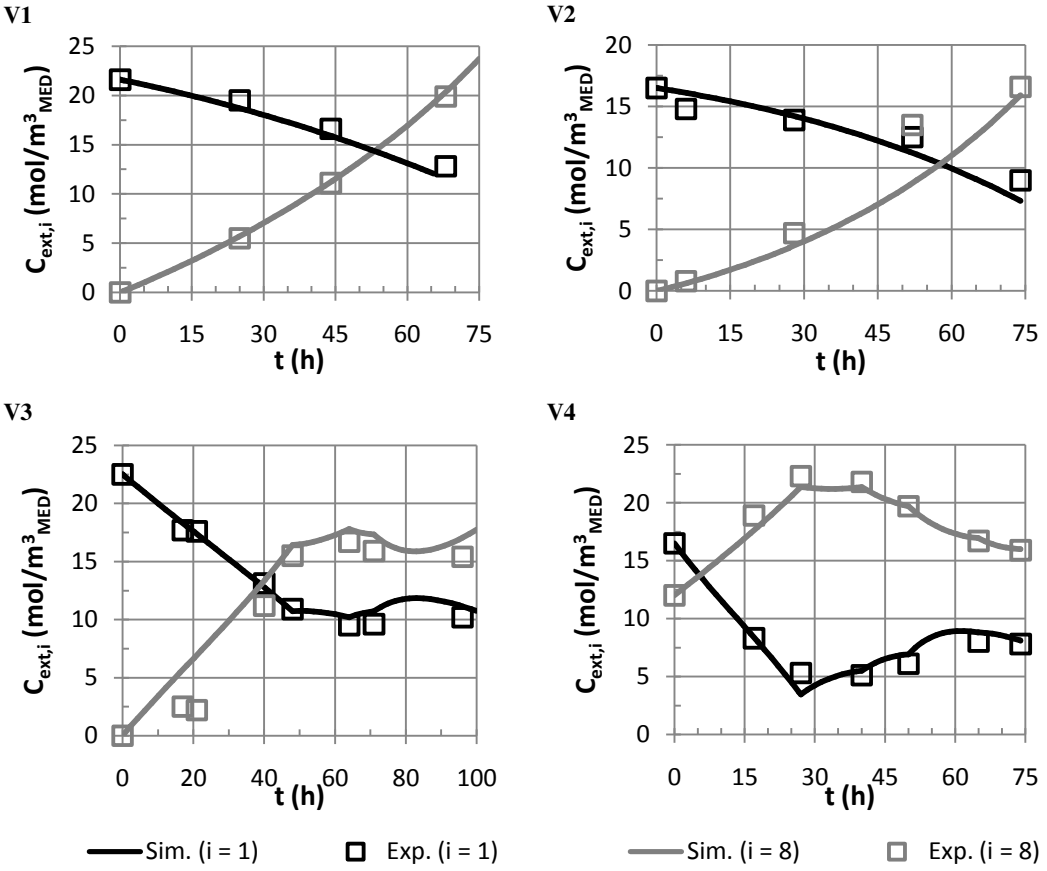

Figure 22 – Computed and experimentally determined time evolutions of the glucose (i=1) and lactate (i=8) concentrations during the cell cultures V1 to V4.

DOI: 10.2202/1934-2659.1534

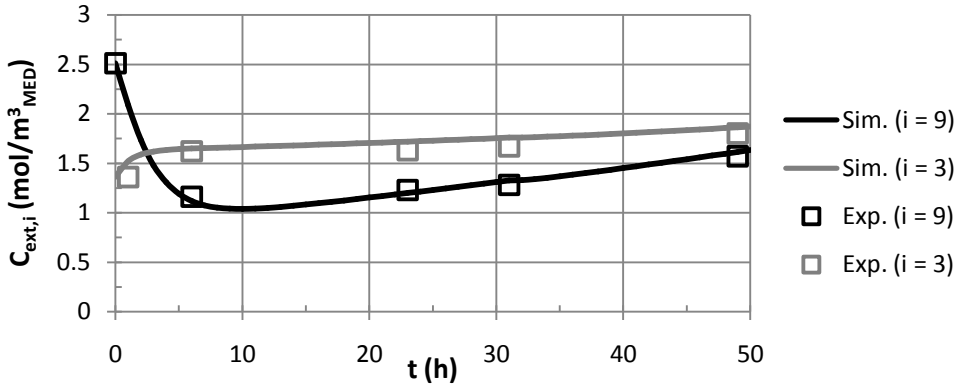

Figure 23 –Computed and experimentally determined time evolutions of the glutamate (i = 3) and ammonia (i=9) concentrations during the cell culture V5.

Table 12 – Time averaged concentrations of glucose (i=1), lactate (i=8) and ammonia (i=9).

Culture	$\mu\ (10^{-2}\mathrm{h}^{-1})$	$C_{\mathrm{ext},1}\ (\mathrm{mol/m^3_{MED}})$	$C_{\mathrm{ext},8}\ (\mathrm{mol/m^3_{MED}})$	$C_{\mathrm{ext},9}\ (\mathrm{mol/m^3_{MED}})$
R1	2.16	11.1	17.4	1.4
V1	2.61	16.5	10.1	1.3
V2	2.61	12.8	6.1	1.3
V3	2.58	14.2	11.9	1.4
V4	1.42	8.0	18.2	1.7
V5	2.08	18.0	15.0	1.4

4. Conclusions

In this work, a structured mathematical model of the VERO cell metabolism in a fixed-bed bioreactor is developed. The mass balance equations for the extra- and intracellular species are written considering the main pathways of the animal cell metabolism.

From this model, the cell metabolism is analyzed. An undetermined set of equations relating the consumption or production rates of the extracellular species and the metabolic reaction rates can be developed. The monitoring of a reference cell culture in a pilot bioreactor enables to transform this undetermined set of equations into a determined one. The resolution of the determined set of equations enables to analyze and characterize the cell metabolism.

From the model and the characterization of the cell metabolism, relations between the concentrations and the consumption or production rates of the extracellular species are identified and introduce in the model to develop a monitoring tool. This monitoring tool enables to simulate the time evolution of the species concentrations when the experimental time evolution of the cell concentration is known. This monitoring tool is used to simulate five cell cultures for the validation of the monitoring tool. The excellent agreement between the

experimentally determined and the computed time evolutions of the species concentrations enables to validate the monitoring tool.

Using the monitor tool, the operating conditions of the cell culture can be selected. For instance, the time averaged concentrations of glucose, lactate and ammonia are computed for the reference culture and for the five cell cultures for the validation of the monitoring tool. For these cultures, the specific growth rate of the cells is also experimentally determined. The inhibitor effect of lactate and ammonia, and the limiting effect of the glucose on the cell growth can be observed. Therefore, the range of the species concentrations can selected for future cell cultures.

The method used to develop the monitoring tool and presented in this work could be applied to another cell line or cell cultures in another bioreactor.

Abbreviations and notations

$\mathrm{aa_E}$	Essential amino acid
$\mathrm{aa_{NE}}$	Non essential amino acid
AcCoA	Acetyl co-enzyme A
αceto	α-cetoglutarate
ADP	Adenosine diphosphate
Ala	Alanine
Asp	Aspartate
ATP	Adénosine triphosphate
CoASH	Co-enzyme A
FB	Fixed-bed
feed	Feeding
G	Glucose
G6P	Glucose-6-phosphate
Gln	Glutamine
Glu	Glutamate
Mal	Malate
OA	Oxalo-acetate
P_{i}	Inorganic phosphate
Pyr	Pyruvate
R5P	Ribose-5-phosphate
TCA	Tricarboxylic acid
VERO	VERvet Origin

$C_{\mathrm{ext,i}}$	Concentration of the extracellular species i	$\mathrm{mol/m^3_{MED}}$
$C_{\mathrm{ext,i,feed}}$	Concentration of the extracellular species i in the feeding medium	$\mathrm{mol/m^3_{MED}}$
$C_{\mathrm{ext,i,*}}$	Saturation concentration of the extracellular species i in the culture medium	$\mathrm{mol/m^3_{MED}}$

DOI: 10.2202/1934-2659.1534

$C_{\text{int,j}}$	Concentration of the intracellular species j	$\text{mol}/(\text{cell m}_{\text{MED}}^3)$
H_{FB}	Height of the fixed-bed	m
$k_{\text{D}}^{\text{eff}}$	Effective kinetic constant of the cell death rate	$\text{m}_{\text{FB}}^3/(\text{cell s})$
$k_{\text{L}}a$	Gas-liquid mass transfer coefficient	s^{-1}
N_{A}	Avogadro's number	cell/mol
$N_{\text{ext,i-n}}$	Stoichiometric coefficient of the extracellular species i in the reaction n	
$N_{\text{int,j-n}}$	Stoichiometric coefficient of the intracellular species j in the reaction n	
$p_{\text{i,0}}$	Zero-order parameter of the polynomial function characterizing the i species consumption or production rate	$\text{mol}/(\text{cell s})$
$p_{\text{i,1}}$	First-order parameter of the polynomial function characterizing the i species consumption or production rate	$\text{mol}/(\text{cell s}^2)$
$p_{\text{i,2}}$	Second-order parameter of the polynomial function characterizing the i species consumption or production rate functions	$\text{mol}/(\text{cell s}^3)$
$p_{\text{i,3}}$	Third-order parameter of the polynomial function characterizing the i species consumption or production rate	$\text{mol}/(\text{cell s}^4)$
Q_{feed}	Flow rate of the feeding medium	$\text{m}_{\text{MED}}^3/\text{s}$
$R_{\text{i=1,n=2}}$	Ratio characterizing the fraction of the glucose implied in the pentose phosphate pathway	
$R_{\text{i=1,n=4}}$	Ratio characterizing the fraction of the glucose implied in the lactic fermentation	
$R_{\text{i=1,n=5}}$	Ratio characterizing the fraction of the glucose implied in the TCA cycle	
$R_{\text{i=9,n=14}}$	Ratio characterizing the fraction of the intracellular produced ammonia implied in the ADN/ARN synthesis	
$R_{\text{i=9,n=12-11-ext}}$	Ratio characterizing the extracellular ammonia produced from aspartate	
$R_{\text{i=9,n=10-ext +10-11-ext}}$	Ratio characterizing the extracellular ammonia produced from glutamine	
RQ	Respiratory quotient	
t	Time	s
$v_{\text{ext,i}}$	Consumption or production rate of the extracellular species i	$\text{mol}/(\text{cell s})$
V_{FB}	Fixed-bed volume	m_{FB}^3
V_{MED}	Medium volume	m_{MED}^3
v_{n}	Rate of the reaction n	$\text{mol}/(\text{cell s})$

X_{FB}	Adhered cell concentration in the fixed-bed	$\mathrm{cell/m_{FB}^3}$
γ	Ratio of the ammonia production rate and the glutamine consumption rate	
μ	Specific growth rate of the cells	$\mathrm{s^{-1}}$

References

Altamirano, C., A. Illanes, S. Becerra, J. J. Cairo and F. Godia (2006). "Considerations on the lactate consumption by CHO cells in presence of galactose." J Biotechnol **125**: 547-556.

Blüml, G. (2007). Microcarrier cell culture technology. Animal Cell Biotechnology: Methods and Protocols. R. Pörtner. Berlin, Humana Press. **24:** 149-178.

Bonarius, H. P. J., V. Hatzimanikatis, K. P. H. Meesters, C. D. d. Gooijer, G. Schmid and J. Tramper (1996). "Metabolic flux analysis of hybridoma cells in different culture media using mass balances." Biotechnol Bioeng **50**: 299-318.

Cerckel, I., A. Garcia, V. Degouys, D. Dudois, L. Fabry and A. O. A. Miller (1993). "Dielectric spectroscopy of mammalian cells." Cytotechnology **13**: 185-193.

Cesco Bioengineering (2010). Culture matrix, macroporous carrier, BioNOC II carriers (Product data sheet), http://www.cescobio.com, 13/04/2010.

Champe, P. C., R. A. Harvey and D. R. Ferrier (2008). Biochemistry. Baltimore, Lippincott Willians & Wilkins.

Darnell, J. E. (1968). "Ribonucleic acids from animal cells." Bacteriol Rev **32**(3): 262-290.

Decker, E. L. and R. Reski (2007). "Moss bioreactors producing improved biopharmaceuticals." Curr Opin Biotech **18**: 393-398.

Drugmand, J.-C. (2007). Characterization of insect cell lines is required for appropriate industrial processes. Ingénierie biologique, agronomique et environnementale, Université Catholique de Louvain. **Ph.D.Thesis**.

Fassnacht, D. and R. Pörtner (1999). "Experimental and theoretical considerations on oxygen supply for animal cell growth in fixed-bed reactors." J Biotechnol **72**: 169-184.

Freshney, R. I. (2005). Culture of animal cells, a manual of basic technique. New Jersey, Willey.

Gartner, L. P., J. L. Hiatt and J. M. Strum (2007). Cell biology and histology. Baltimore, Lippincott, Willams and Wilkins.

DOI: 10.2202/1934-2659.1534

Gelbgras, V., C. Wylock, J.-C. Drugmand and B. Haut (2010). "Segregated model of adherent cell culture in a fixed-bed bioreactor." Submitted to: Chemical Product and Process Modeling.

Haag, J. E., A. Vande Wouver and P. Bogaerts (2005). "Systematic procedure for the reduction of complex biological reaction pathways and the generation of macroscopic equivalents." Chem Eng Sci **60**: 459-465.

Heinrich, R. and S. Schuster (1996). The regulation of cellular systems. New York, Springer.

Huang, H., X. Yi and Y. Zhang (2006). "Improvement of vero cell growth in glutamate-based culture by supplementing ammoniagenic compounds." Process Biochem **41**: 2386-2392.

Huang, H., Y. Yu and X. Yi (2007). "Nitrogen metabolism of asparagine and glutamate in vero cell studied by 1H/15N NMR spectroscopy." Appl Microbiol Biot **77**: 427-436.

Invitrogen (2010). OptiPRO SFM (Product data sheet, Form No. 3943), http://www.invitrogen.com, 13/04/2010.

Jang, J. D. and J. P. Barford (2000). "An unstructured kinetic model of macromolecular metabolism in batch and fed-batch cultures of hybridoma cells producing monoclonal antibody." Biochem Eng J **4**: 153-168.

Jolivet, E., J. D. Lebreton, C. Millier, A. Pavé and J. P. Vila (1982). Modèles dynamiques déterministes en biologie. Paris, Masson.

Kilberg, M. S. and D. Häussinger (1992). Mammalian amino acid transport: mechanisms and control. New York, Kluwer Academic.

Klamt, S. and J. Stelling (2003). "Two apporaches for metabolic pathway analysis ?" Trends Biotechnol **21**(2): 64-69.

Lehningher, A. L. (1977). Biochimie, bases moléculaires de la structure et des fonctions cellulaires. Bourges, Flammarion.

Martens, D. E. (2007). Metabolic Flux Analysis of Mammalian Cells. Systems Biology. S. Netherlands. **5:** 275-299.

Matsuoka, H. and T. Takeda (2005). Effet of glucose and glutamine concentration on metabolism of animal cells in chemostat culture. European Society for Animal Cell Technology 18th, Granada, Spain, Proceedings.

Mendonça, R. Z. and C. A. Pereira (1998). "Cell metabolism and medium perfusion in VERO cell cultures on microcarriers in a bioreactor." Bioprocess Eng **18**: 213-218.

Meuwly, F. (2006). Characterization of fibra-cell® packed bed bioreactors for the culture of CHO cells. Institut des Sciences et Ingéniérie Chimiques, Ecole Polytechnique Fédérale de Lausanne. **Ph.D.Thesis**.

Möhler, L., A. Bock and U. Reichl (2008). "Segregated mathematical model for growth of anchorage-dependent MDCK cells in microcarrier culture." Biotechnol Progr **24**: 110-119.

Nova Biomedical (2010). BioProfile Analyser, http://www.novabiomedical.com, 13/04/2010.

Okayasu, T., M. Ikeda, K. Akimoto and K. Sorimachi (1997). "The amino acid composition of the mammalian and bacterial cells." Amino Acids **13**: 379-391.

Provost, A. and G. Bastin (2004). "Dynamic metabolic modelling under the balanced growth condition." J Process Contr **14**: 717-728.

Ricklefs, R. E. and G. L. Miller (2003). Ecologie. Bruxelles, De Boeck.

Rios-Estepa, R. and M. B. Lange (2007). "Experimental and mathematical approaches to modeling plant metabolic networks." Phytochemistry **68**: 2351-2374.

Sanderson, C. S., J. P. Barford, G. W. Barton, T. K. K. Wong and S. Reid (1999). "A structured model for animal cell culture: application to baculovirus/insect cell systems." Biochem Eng J **3**: 219-229.

Schneider, M., I. W. Marison and U. v. Stockar (1996). "The importance of ammonia in mammalian cell culture." J Biotechnol **46**: 161-185.

Seth, G., P. Hossler, J. Chong Yee and W.-S. Hu (2006). "Engineering cells for cell culture bioprocessing - Physiological fundamentals." Adv Biochem Biot **101**: 119-164.

Street, J. C., A.-M. Delort, P. S. H. Braddock and K. M. Brindle (1993). "A 1H/15N n.m.r study of nitrogen metabolism in cultured mammalian cells." Biochem J **291**: 485-492.

Voet, D., J. G. Voet and G. Rousseau (2005). Biochimie. Bruxelles, De Boeck.

Warnock, J. N., K. Bratch and M. Al-Rubeai (2005). Packed bed bioreactors. Bioreactors for Tissue Engineering. Dordrecht, Springer Netherlands**:** 87-113.

Xiu, Z.-L., W.-D. Deckwer and A.-P. Zeng (1999). "Estimation of rates of oxygen uptakes ans carbon dioxide evolution of animal cell culture using material and energy balances." Cytotechnology **29**: 159-166.

Zupke, C. and G. Stephanopoulos (1995). "Intracellular flux analysis in hydridomas using mass balance and in vitro 13C NMR " Biotechnol Bioeng **45**: 292-303.

DOI: 10.2202/1934-2659.1534